International Journal of Engineering Research & Technology (IJERT)
ISSN: 2278-0181
Vol. 15 Issue 07 , July - 2026

Aerodynamic Analysis of Wing with Fence System

J. Jayanth
24951D7602
Master of Technology
Department of Aeronautical Engineering
Institute Of Aeronautical Engineering
Dundigal, Hyderabad – 500 043, Telangana

Abstract - The aerodynamic performance of finite wings is strongly affected by spanwise flow and wingtip vortices, which contribute to increased drag and reduced efficiency. This study aims to carry out a computational analysis of a tapered wing designed based on NACA 64A008 airfoil using a wing fence system as a passive flow control device. The wing geometry has a root chord of 100 mm, tip chord of 75 mm and a taper ratio of 0.75. The aerodynamic analysis is performed using ANSYS Workbench and steady state simulation in ANSYS Fluent is performed with the thickness of the wing fences of 2 mm and 3 mm, and their positions are 200 mm, 250 mm and 300 mm away from the root of the wing. The applied inlet velocity is 31.725 m/s which is a low Reynolds number flow and the angle of attack is kept constant at 3deg. The comparative study is made between baseline wing (without fence) and modified wing with fence configuration to study the effect of placing the fence and thickness of the fence on the aerodynamic performance.The results show that the introduction of wing fences has a major effect on the flow structure, in lowering the spanwise flow and diminishing the tip vortices. This results in better lift performance and decreased wing surface flow separation. By examining the fence configurations, it was found that the fenced wing configuration has a better L/D ratio than the baseline configuration and that there are optimal fences configurations for optimum L/D ratio performance.The findings of this study demonstrate the effectiveness of wing fences as one of the passive flow control mechanisms to enhance the aerodynamic efficiency and also give valuable insights for their use in wing design and optimization of aircraft.

Keywords : Aerodynamic Analysis , Wing Fence System , ANSYS Fluent , NACA 64A008 Airfoil , Flow Separation , Low Reynolds Number Flow , Boundary Layer Behavior Flow Separation

NOMENCLATURE

AOA- Angle of Attack

CFD – Computational Fluid Dynamics

PIV – Particle Image Velocimetry

Symbols:

C = Airfoil chord length, m.

C_d = Drag coefficient

C_l = Lift coefficient

C_p = pressure coefficient

F_1 = blending function in the shear-stress transport model

k = turbulent kinetic energy, m^2/s^2

L = length, m

N = amplification factor

p = pressure, $kg/m\cdot s^2$

P_k = turbulent kinetic energy production rate, $kg/m\cdot s^3$

Re = chord-based Reynolds number

International Journal of Engineering Research & Technology (IJERT)
ISSN: 2278-0181
Vol. 15 Issue 07 , July - 2026

Re_θ = momentum-thickness Reynolds number, $\rho\theta U_\infty/\mu$

$Re_{\theta t}$ = freestream transition-onset momentum-thickness Reynolds number, $\rho\theta_t u/\mu$

$\check{R}e_{\theta t}$ = local transition-onset momentum-thickness Reynolds number, $\rho\theta_t u/\mu$

Re_υ = strain-rate Reynolds number

S = strain-rate magnitude, $2(S_{ij}S_{ij})^{0.5}$; strain-rate tensor, $0.5(\partial U_i/\partial x_j+\partial U_j/\partial x_i)$

t = time, s

Tu = turbulence intensity, $100(2k/3)^{0.5}/U$

U = freestream velocity, m/s

u = local velocity, m/s

α = Angle of attack

γ = intermittency

θ = momentum thickness, m

μ = dynamic viscosity, kg/m· s

μ_t = eddy viscosity, kg/m· s

ρ = density, kg/m^3

τ_w = wall shear stress, kg/m· s^2

υ = kinematic viscosity, μ/ρ, m^2/s

ω = turbulent eddy frequency, s

CHAPTER 1

INTRODUCTION

1.1 Understanding Spanwise Flow and the Need for Wing Fences

The wing fence is a passive aerodynamic device as opposed to other flap or slat systems, and does not need to be powered. It acts as a physical obstruction to spanwise (lateral) airflow across the wing, mainly at high angles of attack.

From a visual perspective, a fence is usually arranged to follow the shape of the airfoil, around the front and extended towards the aft end. Though their simplicity, they are the outcome of intricate fluid dynamics and are designed to solve the instabilities of swept-wing des The Genesis of the Problem: Spanwise Flow inherent in such wings.

The "swept-wing penalty" is a fundamental element of fences that must be understood. Today, in aviation, wings are swept back to defer the occurrence of wave drag at high speeds. This sweep causes, however, a pressure gradient that causes the boundary layer (that layer of air that adheres to the wing surface) to flow sideways--from the root (near the fuselage) to the tip.

As the air moves towards the tip, the boundary layer increases and loses energy. This causes "stagnant" air to collect at the tips of the wings. This is because the air at the tips of the wing stalls at a lower angle of attack than the air at the base of the wing, when the aircraft slows down or when it angles up, like during takeoff or landing.

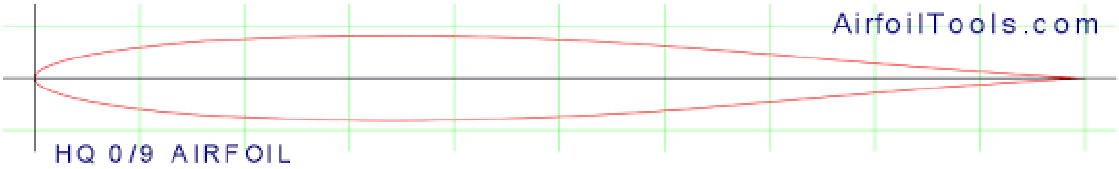

Figure 1.1 : Airfoil Tools

International Journal of Engineering Research & Technology (IJERT)
ISSN: 2278-0181
Vol. 15 Issue 07 , July - 2026

The basic aerodynamic concept of a wing fence is the disintegration of the transverse pressure gradient. Swept wing lines of constant pressure (isobars) do not run parallel to the leading edge. The fence is a 'dam' that stops the low energy boundary layer from traveling toward the wingtip.

The fence itself directs the airflow in a chordwise direction (straight down the wing), allowing the "cleaner," higher energy air to flow through the outboard portions of the wing. This keeps the wingtip effective for longer in high pitch manoeuvrings.

1.2 Vortex Generation and Re-energization

In addition to being a barrier, modern aerodynamic theory indicates that fences operate as vortex generators as well. If the angle of attack is large, air will spill over the top of the fence to form a controlled vortex. This vortex can be likened to a "mixer", which draws high energy air into the slow-moving boundary layer. It is called boundary layer re-energization and causes even more delay in the onset of a stall.

The impact on flight stability and control is discussed below.The effect on flight stability and control is summarized below.

There are steps that can be taken to prevent the "Pitch-Up" Phenomenon.

Early swept wing jets had a tendency to pitch up which made them one of the most dangerous features. In a swept wing aircraft, the first wing stall is at the tips, causing the Center of Pressure (CP) to move forward and towards the fuselage (inward). The tips are aft of the aircraft's Center of Gravity (CG) which will cause the nose to pitch up violently when the air is lost at the tail.

This is prevented by a wing fence:

- Having the wingtip stay at a higher angle of attack than the root.Keeping the wingtip at a higher angle of attack than the root.
- Making sure that, if there is a stall, it is symmetrical and predictable.
- Keeping the nose stable by keeping its downward force or lift balance.

Aileron Effectiveness

Ailerons are usually attached near the wingtips to give the pilot the maximum roll moment. In the event of wingtip stall caused by spanwise flow, the pilot loses roll control at the very time it is most needed--when landing at low speed. The fence keeps the flow attached on the outside of the wing, which means the ailerons are “alive” and responsive.

1.3 Design variations and placement strategy.

Chordwise Extension

It is uncommon to find a fence that is laid out across the full chord of the wing. The majority of fences start at the front and sweep over 50% to 80% of the chord. Fences should be pushed to the rear end of the aircraft if they are being used for stalling, but not if they are being used for drag.

Height and Thickness

Typically, the height of a fence is fixed by the thickness of boundary layer at the "critical" angle of attack of the design. Too short and the air will simply jump the fence, too tall and during high-speed cruise too much parasitic drag will be created.

Strategic Positioning

Fences are generally located around the mid-span or inboard edge of the ailerons where the boundary layer starts to become appreciably thick. Other planes, such as the MiG-17 or the Sud Aviation Caravelle, employed two or more fences to control the flow, stage by stage throughout the span.

The student will compare and contrast fences to other devices

To appreciate the wing fence, it must be compared to its aerodynamic "cousins":

International Journal of Engineering Research & Technology (IJERT)
ISSN: 2278-0181
Vol. 15 Issue 07 , July - 2026

Device	Mechanism	Primary Advantage	Disadvantage
Wing Fence	Physical barrier/Vortex	Simple, no moving parts	Adds parasitic drag at cruise
Vortex Generators	Small tabs creating vortices	Lightweight, very targeted	Effective only in specific areas
Leading Edge Slats	Redirects high-pressure air	Extremely effective lift boost	Heavy, complex, mechanical
Dogtooth/Sawtooth	Discontinuity in leading edge	Generates strong vortex	Fixed geometry affects all speeds

Table 1 : Fence Vs other devices

The fence is a common choice, where an intermediate solution is required, which means a higher flow control than a vortex generator, yet without the weight and maintenance burden of a retractable slat.

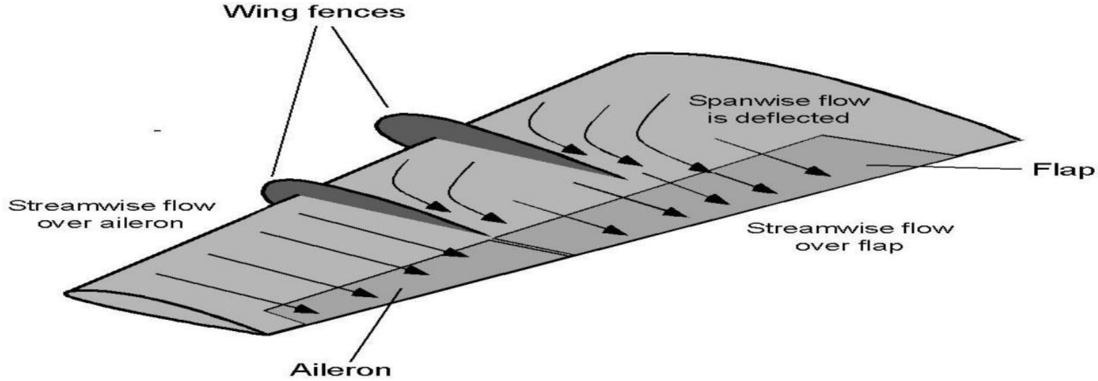

Figure 1.2: Wing with Fence [2]

1.4 Historical Evolution and Modern Usage

The Cold War Era

The 1950s and 60s represented the "Golden Age" of the wing fence. As jet engines allowed for faster speeds, wing sweeps became more aggressive. Soviet engineers, in particular, favored large, prominent fences on the MiG-15, MiG-17, and MiG-19 series to counter the treacherous handling qualities of their highly swept wings.

Transition to Modern Aerodynamics

In modern commercial aviation, you see fewer large wing fences. This is due to the advancement of **Supercritical Airfoils** and **3D Wing Design**. Engineers can now "twist" the wing (washout) or change the airfoil shape along the span to naturally discourage spanwise flow.

However, fences are still found on:

International Journal of Engineering Research & Technology (IJERT)
ISSN: 2278-0181
Vol. 15 Issue 07 , July - 2026

- **Business Jets:** Where wing sweep is necessary but cost/weight must be kept low.
- **STOL (Short Take-Off and Landing) Aircraft:** Where low-speed performance is the highest priority.
- **Retrofits:** When an existing wing design shows unexpected stall characteristics during flight testing, a fence is often the most cost-effective "fix.

Low Reynolds number

The dominance of viscous forces over inertial forces is shown by a low Reynolds number. As a consequence, the fluid moves in a smooth and continuous pattern known as laminar flow. When the Reynolds number is less than 2000, we say that the flow is internal or occurring in a closed environment. When the Reynolds number is less than 1100, the flow is considered laminar. As soon as the Reynolds number goes over 2200, the flow becomes turbulent. In the case of external flows where the fluid has a bigger space of flow over a body with a confined volume the Reynolds number value given for that fluid flowing around the body is 100000.Any Reynolds number value considered below the mentioned value is external flow with a low Reynolds number and above the mentioned value is high Reynolds number value. So comes the flow characteristics for the fluid medium flowing around the body [1].

Low Reynolds number flow physics

Flows with a low Reynolds number are those in which the role of inertia in influencing the motion is minimal. Where μ denotes viscosity and ρ denotes density, the formula for the Reynolds number of a fluid is "$R = \rho VL/\mu$".

Relyon velocities that are low suggest that:

- To a far greater extent than inertial forces, viscous forces
- A laminar flow is one in which the velocity profile is flat and undistorted.
- Viscosity is the primary determinant of the fluid's behavior.
- The flow may be described as laminar, steady, smooth, or viscous.

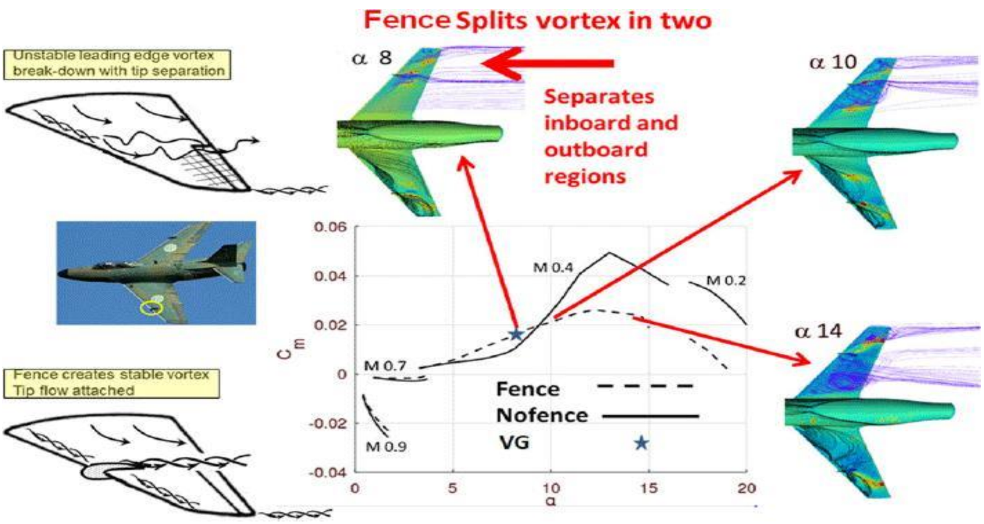

Figure 1.3 Wing Simulation [2]

A low Reynolds number flow is a typical flow with flow having viscous force greater than the inertial forces. When fluids have mechanical qualities like density, which pack the fluid layers together to create a thick fluid layer, the result is viscosity, which is the resistance to the flow direction of the fluid. The inertial forces acting on a body are its characteristic length, the fluid's density, and the fluid's velocity.

When this flow equals 100,000 its typically called transition high Reynolds number flows, the flow Reynolds number value, when observed to be less than this it’s usually called a low Reynolds number flow for external flows. To understand it more deeply, the

International Journal of Engineering Research & Technology (IJERT)
ISSN: 2278-0181
Vol. 15 Issue 07 , July - 2026

inertial forces of the flow are so less that they are causing a very little difference in ratio over the opposing viscous forces over the characteristic length of the body .

1.5 Flow control techniques

Flow control techniques have been developed by careful examination of flows and understanding different insights gained over both computational data and experimental investigation of different fluid behaviours at different flow conditions.

Flow control strategies may be broadly categorized into two groups: passive and aggressive.

Some examples of passive approaches include the Gurney flap, vortex generator, bump, cavity, roughness, minor disturbance, bleed, splitter plate, polymer, and biomimetic techniques.

Acoustic excitation, jets, synthetic jets, plasma actuators, Lorentz forces, and oscillation and flow perturbation are some of the active ways.

1.5.1 Methods for active flow control

The use of energy-hungry actuators, some of which may have time-dependent operations, is essential for active control. Using synthetic jets, valves, plasma actuators, and constant or unstable suction or blowing are all examples of active flow control. Both open-loop control, in which actions are predetermined, and closed-loop control, in which actions are reliant on sensors for monitoring, are possible [3].

Re, or Reynolds Number,

When trying to foretell how a fluid will move through a given system, fluid mechanics turn to the dimensionless Reynolds number (Re). This comparison between inertial and viscous forces helps to identify the flow type, which might be laminar, transitional, or turbulent.Mathematically Calculated using:

$$Re = \frac{\rho \times v \times L}{\mu} \qquad (1.1)$$

Where:

Re- Reynold's number,

ρ- Density of fluid,

v- Velocity of fluid,

µ- Dynamic viscosity,

L - Characteristic length

The Reynolds number is a very important parameter in fluid dynamics and finds multiple practical uses, such as:

Flow behaviour prediction: The Reynolds number can be used by engineers to predict how the flow will be laminar, transitional or turbulent across various fluid systems.

Design optimization: Design engineers can learn to optimize fluid flow systems, including pipes, channels, and surfaces in aerodynamics, by comprehending the flow regime to attain the desired characteristics of performance.

Aerodynamics: Reynolds number is essential in aerodynamics to assess airflow over aircraft wings, propellers, and other surfaces.

Heat transfer: Reynolds number plays a role in heat transfer calculations, such as determining the onset of natural convection or the design of heat exchangers.

International Journal of Engineering Research & Technology (IJERT)
ISSN: 2278-0181
Vol. 15 Issue 07 , July - 2026

Figure 1.4 : Wing of aircraft

Coefficient of lift (C_l)

An airfoil's or wing's lift may be described by a dimensionless quantity called the coefficient of lift (Cl). It is defined as the ratio of the lift force acting on the airfoil to the dynamic pressure multiplied by the reference area of the airfoil.

The following equation may be used to compute the lift coefficient:

$$C_l = \frac{Lift\ force}{\frac{1}{2} \times \rho_{air} \times V^2 \times A} \quad (1.2)$$

V is the fluid velocity relative to the object, ρ is the fluid density, and A is the reference area. The formula uses the airfoil's reference area, which is perpendicular to the direction of the airflow, the airfoil's velocity (V), and the density of the air passing through it. A multitude of variables, including airfoil form, speed, Reynolds number, and angle of attack, influence the coefficient of lift. Coefficients of lift tend to rise with increasing angles of attack until they reach a maximum, and then they start to fall. A stall angle of attack is this. Keep in mind that the lift coefficient is not a fixed number; it is dependent on the airflow conditions and can change significantly depending on the operating conditions of the airfoil.

Coefficient of drag (C_d)

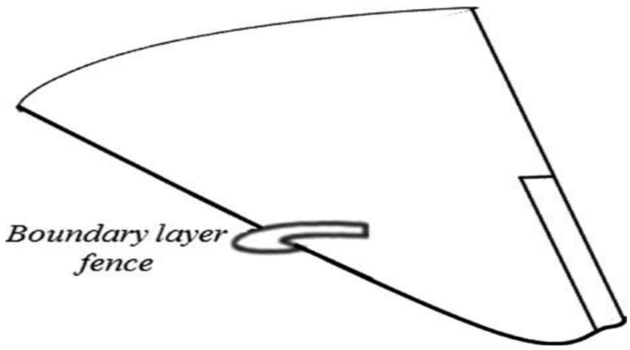

Figure 1.5 Boundary layer fence

When an item is in motion through a fluid like air, it experiences aerodynamic drag, which is represented by the dimensionless coefficient of drag (Cd). Aerodynamics makes use of it to measure the amount of resistance an item experiences when traveling through a fluid. An object's drag force, Fd, is equal to the ratio of the fluid's dynamic pressure, 1/2 × ρ × V2, to the object's reference area, A. Mathematically, it can be expressed as:

$$C_d = \frac{Drag\ force}{\frac{1}{2} \times \rho_{air} \times V^2 \times A} \quad (1.3)$$

International Journal of Engineering Research & Technology (IJERT)
ISSN: 2278-0181
Vol. 15 Issue 07 , July - 2026

V is the fluid velocity relative to the object, ρ is the fluid density, and A is the reference area. Common examples of reference areas are cylinder cross-sections and airfoil planforms, which are maximally projected in a direction perpendicular to the direction of fluid flow. Several variables come into play here, including the object's form, surface roughness, fluid density and velocity, and the angle of attack, which is defined as the angle between the object's chord line and its velocity. A smooth and thin shape tends to produce a smaller coefficient of drag whereas rough surfaces and non-streamline shapes tend to add drag. In aerodynamics, the coefficient of drag is an important parameter for design and analysis, because it influences how well planes fly and how much fuel they use, automobiles, and other objects that move through a fluid. Reducing the coefficient of drag can result in improved speed and fuel efficiency. Understanding and controlling the coefficient of drag is therefore a critical aspect of aerodynamic design and engineering.

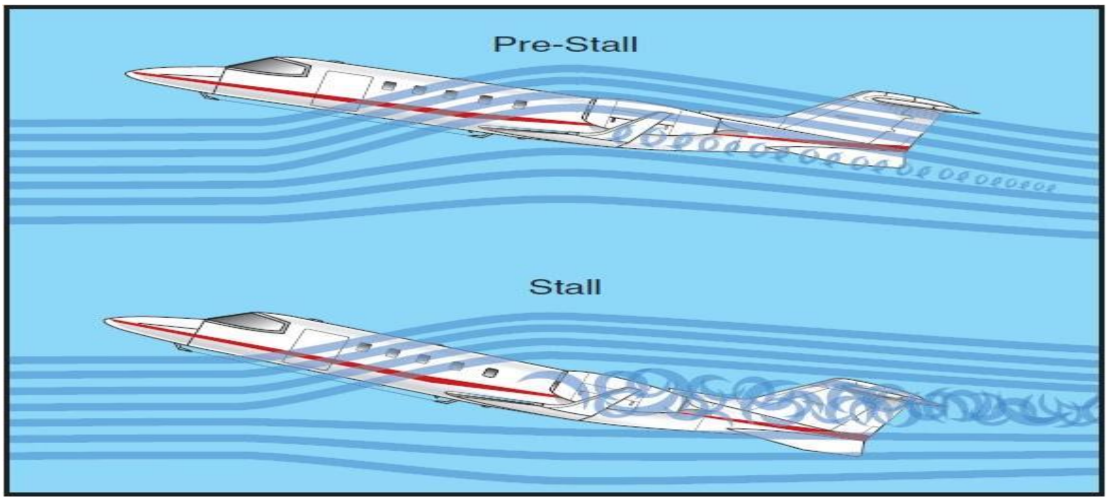

Figure 1.6 Stall Images [4]

Stall is observed on a wing when the separation layers don't meet at the end of the surface of the body. This is more prone to in slower flows such as low Reynolds number flows. To reduce the feasibility of this phenomenon different methods such as Cavitation have to be used to improve the flow around the body and mitigate the shear layer separation.

1.6 Objective of project work

To test, compare a particular flow control technique called cavitation to improve the performance characteristics of the airfoil body. To test and verify the most possible simplest geometry cavity for an airfoil to cause significant increase in lift and decrease in drag. To observe the particular change in the flow due to cavity around the body.

1.7 Organisation of thesis

Thesis organised basing on the work flow followed, starting with the initial research and gaining a full understanding about the phenomenon and the causes and appropriate solutions for that. Followed by a selection of reference for carrying on a research methodology. The research methodology needs validation before proceeding with the research. Once the validation is over the actual research process starts. Preprocessor stage handling the initial process of research flow, constructing mesh geometry and making suitable changes as per the need. The next step is to consider meshing the geometry as per requirement, the mesh is made and is tested for mesh errors and mesh independency is studied. The actual solution starts as the mesh is subjected to flow type Reynolds number 10000 steady flow. The same solution is run for many angles of attack of the fluid throughout the domain. The results are then recorded and analysed for getting a deeper understanding of the fluid behaviour around the airfoil body. All the results are carefully analysed to come up with an understanding and conclude the product of approach utilised in the research work.

The Aerodynamic Genesis of Spanwise Flow andThe High-Speed Imperative: Wing Sweep

The transition from straight wings to swept wings was necessitated by the "Sound Barrier." As aircraft approached Mach 1, straight wings experienced massive wave drag. The drag was delayed by sweeping the wings in a backward (USD 25 0 USD 45 0 USD) direction, but this caused a flow problem which was three dimensional.

The Cross-Flow Component

International Journal of Engineering Research & Technology (IJERT)
ISSN: 2278-0181
Vol. 15 Issue 07 , July - 2026

On a swept wing, the wing air velocity vector (USD V\inftyUSD) can be broken down into two components:

1. Chordwise Component (USD VcUSD): Moves normal to the leading edge; lift cause.

2. Spanwise Component (USD VsUSD): Motion perpendicular to the leading edge to the wingtip.

The larger the angle of attack (USD \alphaUSD), the larger is the spanwise component. This scoots the low-energy boundary layer along to the wingtips and the result is a huge concentration of stagnant air at the very section of the wing that provides roll control (the ailerons).

Physics and Anatomy of the Fence System. The "Damming" Effect

Fence is a mechanical demarcation. It prevents the spanwise movement of the boundary layer thereby forcing the air to remain localized to its chord section. This keeps the tip thickening its boundary layer too late, otherwise causing an early stall.

Vortex Filament Theory

At the fence, when the air hits the fence at a high USD \alphaUSD, the difference between the pressure on the inboard and outboard side of the fence causes the air to roll over the top edge. This forms a Longitudinal Vortex concentrated.

Mechanism: This vortex is a "fluidic fence," higher still than the metal plate itself.

Re-energization: It has the high-momentum air in upper atmosphere flow being pulled down to the level of the surface cleaning out the stagnant air.

1.8 Mathematical model and CFD analysis.

The Navier-Stokes Approach

However, we usually solve Reynolds-Averaged Navier-Stokes (RANS) equations in modern analysis (as we have seen in the screenshots of Ansys Fluent above). The fence is implemented as a “No-Slip” boundary condition.

Turbulent Modeling (SST USD kUSD -USD \omegaUSD)

The industry standard in the research of fences is the Shear Stress Transport (USD SSTUSD) USD kUSD -USD \omegaUSD -USD model, which is a combination of:

The accuracy of the USD kUSD -USD \omegaUSD model close to the wall (the fence surface).

The accuracy of the USD kUSD -USD \epsilonUSD model in the free stream (the air well distant off the wing).

Lift and Drag Polar Shifts.

The Lift Curve Slope is altered by a fence. In the absence of a fence, the USD CLUSD vs. USD \alphaUSD curve decreases drastically at the stall point. The curve is smoothed out with a fence, which offers a more predictable stall, with some room to maneuver, to the pilot.

Comparative Research: Fences vs. Modern Control of flows.

The "Dogtooth" Extension

A dogtooth is a stinging notch in the fore-edge. It has been found to leave a vortex like that of a fence though not as effective as blocking the physical migration of the boundary layer.

Vortex Generators (VGs)

International Journal of Engineering Research & Technology (IJERT)
ISSN: 2278-0181
Vol. 15 Issue 07 , July - 2026

Whereas a fence is a single large plate, VGs are dozens of smaller ones. It has been shown that a VGs is more effective in repairing a small, local point of separation and a fence is more effective in controlling the stability of the whole wing span throughout the world.

1.9 Historical Studies and Case Studies.

The NACA 2495 Reports (1950s)

The first systematic tests were done by the National Advisory Committee for Aeronautics (NACA). They discovered that with a wing that is USD 35oUSD swept, a fence at 60 percent of the semi-span gave the best compromise between stall protection and drag.

Soviet TsAGI Innovations

The Soviet scientists discovered that fences performed better as wings became very thin profiled (supersonic jets) compared to slats since they did not need internal hydraulics to work, thus saving mass and giving the wing more capacity to carry more fuel.

1.10 Design Optimization Parameters

Engineers work on the following four variables to fill in the remaining A4 pages of a report:

Length of Chord: Typically half to two-thirds the chord of the wing.

Height (USD hUSD): A typical is USD 1 0 USD to USD 5 0 USD of the local chord length (USD cUSD).

Position: Placing Position The position is generally just inboard of the ailerons to shield the roll control.

rap-around: Leading-edge wrap-around designs are better with the low-speed landing configurations.

Computational Analysis Procedure (The "How-To")

For a detailed analysis, the researcher follows these steps:

1. **Geometry Generation:** Create the 3D airfoil and fence Catia V5
2. **Meshing:** To capture the physics of the boundary layer, apply "Inflation Layers" around the fence.
3. **Boundary Conditions:** Set the "Inlet" velocity to the desired Mach number and "Outlet" to atmospheric pressure.
4. **Post-Processing:** Use **Streamlines** to visualize if the air is successfully staying chordwise or if it is still leaking over the fence.

Future: Active and "Morphing" Fences

Recent research at Boeing and NASA suggests that a "fixed" fence is inefficient during cruise. New papers explore:

Retractable Fences: Only deploy during takeoff and landing.

Fluidic Fences: Using "Air Knives" (thin sheets of blown air) to create a barrier that can be turned off to eliminate drag during high-speed flight.

CHAPTER 2

LITERATURE SURVEY

Aircraft like airplanes that can soar through the air thanks to their fixed wings and the lift they provide are known as fixed-wing aircraft. In aerodynamics and aviation, a stall occurs when the angle of attack is too high, causing the lift to start decreasing. The crucial angle of attack is the inclination at which this happens. The critical angle for subsonic airfoils is usually between 8 and 20 degrees relative to the incoming wind, however it may vary depending on the wing's airfoil section or profile, platform, aspect ratio,

International Journal of Engineering Research & Technology (IJERT)
ISSN: 2278-0181
Vol. 15 Issue 07 , July - 2026

and other variables. In contrast to wing, which improve aerodynamic efficiency by attempting to recoup vortex energy, they prevent the whole wing from stalling simultaneously by blocking span-wise airflow along the wing. An aircraft's performance and fuel efficiency may be greatly enhanced with a redesign of the winglets. Although winglets may make a wing with less drag, they make the structure more complicated and expensive. Furthermore, they alter the qualities of handling and stability. If we look at the drag breakdown of a normal transport plane, we can see that lift-induced drag accounts for 80-90% of the drag during takeoff and up to 40% during cruising. Lift, drag, weight, and thrust are the critical characteristics that control the aircraft's performance. Improving the aerodynamic design, reducing weight, and upgrading systems (such as an engine, fuel system, etc.) may provide the desired performance. The subtended angle of the fence is 10–30 degrees, and the Reynolds number is 20–100. The distance between the neck and the fence may range from 0.2 to 2.6. Multiple aspects have been uncovered by studying the effects of offense subtended angle, fence placement relative to the throat, and Reynolds number on conventional diffuser qualities. Researchers also examine the aerodynamic and aeroacoustic impacts with the use of flat barriers.

2.1 Why Wing Fence Is Beneficial

By reducing generated drag by as much as 20%, a wing fence may save engine power and fuel consumption by 10% to 12%.

• Enhances an airplane's performance metrics, such as its range, climbing rate, time of ascent, etc. Section II: Wing Engineering Through the use of CATIA V5, the wing and wing fence model have been designed. In order to mesh all of those models, ANSYS workbench was used. To get the results of the flow study, the last analysis was done in ANSYS CFX. The four-digit series wing model was a NACA 0012, measuring 30 cm in wing span and 10 cm in chord length. The dimensions of the fence are identical to those of the airfoil, which has a height of just 1 cm, a thickness of around 1.25 mm, and a length of no more than 70% of the chord. Initially work was taken in plain or base airfoil to find out the stalling angle. Once the stalling angle was found out, then the next step is to carry out our investigation in single fence with wing and two fences with wings.

The current analysis's boundary conditions will be discussed in this section. For a constant Reynolds number, a velocity inlet is used at the boundary's inlet with a free stream velocity of 30 m/s. If the wing section has a noslip boundary condition, it is treated as a solid wall. The typical wall functions are used to choose the turbulent model from k-w. At a free stream velocity of 30 m/s, the values of the lift and drag coefficients of the wing section are predicted using computational analysis. The ANSYS CFX post is thus the source of the axial and normal forces. The equation $L=N\cos\alpha - A\sin\alpha$ and the related differential equation $D=A\cos\alpha + N\sin\alpha$ are identical. Following that, the coefficient of lift (CL) and coefficient of drag (CD) are determined by dividing the length (L) by the product of half of the square of the velocity (ρ) and the area (V2*S).

2.2 Result And Discussion

What follows is an analysis of how the lift and drag coefficients change with respect to the varied attack angles. At first, we determined the stalling angle by working on the basic airfoil.

S.NO	ANGLE OF ATTACK	BASE AIRFOIL (C_L)	BASE AIRFOIL (C_D)
1	0	0	0.01856387
2	10	1.0047479	0.236858582
3	11	1.071806113	0.28114351
4	12	1.136190887	0.321926252
5	13	1.075538189	0.357173418
6	15	0.819103571	0.425733763

Table 2 : Various angles of attack of Base airfoil

International Journal of Engineering Research & Technology (IJERT)
ISSN: 2278-0181
Vol. 15 Issue 07 , July - 2026

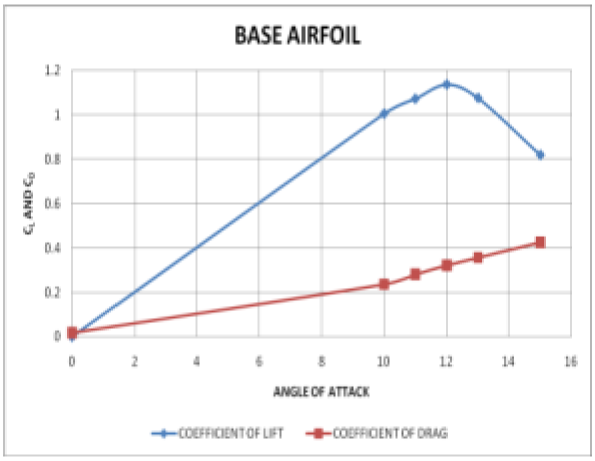

Graph 1 : Base airfoil at 13° angle of attack

Various angles of attack (0, 10, 11, 12, 13, and 15 degrees) and a constant speed of 30 meters per second were used in the basic airfoil work. The base airfoil stalls at an angle of attack of thirteen degrees and has a maximum lift coefficient of one and one-third.

2.3 Contours that are Pressure Coefficient

On each side of NACA 0012, the pressure distribution ranged from zero degrees to twenty degrees.

ANGLE OF ATTACK	SINGLE FENCE (C_L)	TWO FENCE (C_L)	SINGLE FENCE (C_D)	TWO FENCE (C_D)
0	6.04686E-05	6.04686E-05	0.0225548	0.024187453
10	1.050953143	1.033652487	0.23597782	0.23415607
12	1.236050225	1.222102446	0.329366772	0.3275148
15	1.43077935	1.402493769	0.482453485	0.475876336
20	1.478293551	1.477961578	0.723192816	0.727640381
21	1.226658661	1.142199444	0.739783704	0.744022271

Table 3 : Various angles of attack of Single fence and two fence

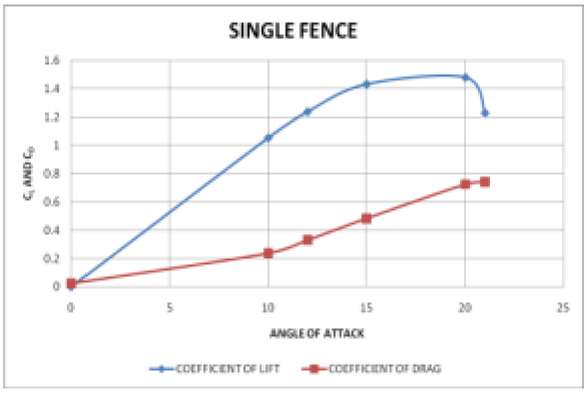

Graph 2: Calculating CL and CD for an airfoil with a single bar

Work was done in the single-fence airfoil at a constant speed of 30 m/s with varying angles of attack ranging from 0 to 21 degrees. At an angle of attack of 21 degrees, this single-fence airfoil stalls with a maximum lift coefficient of 1.478. The insertion of the fence with these specifications has a bigger impact, increasing both the lift and the stalling angle, which results in higher variety.

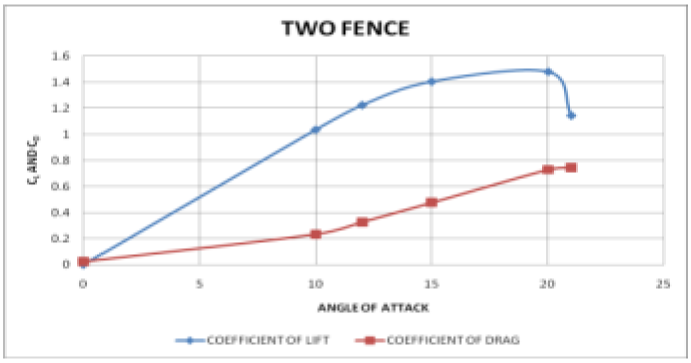

Graph 3: CL and CD for a two-fence airfoil

Work was done in the single-fence airfoil at a constant speed of 30 m/s with varying angles of attack ranging from 0 to 21 degrees. At an angle of attack of 21 degrees, this single-fence airfoil stalls with a maximum lift coefficient of 1.477. This produces results that are comparable to those of a single fence, with the exception that the lift coefficient is somewhat lower and the drag coefficient is slightly higher.

The storied past of wing fence and its many impacts on aerodynamic performance are fascinating. Its previous users include the MiG-15 and F-38, while its most current users include the Fiat G91, BAe Hawk, and Harrier. Situated perpendicular to the wing surface and parallel to the aircraft's longitudinal axis, a wing fence is just a flat plate. The mechanism was first installed on the Messerschmitt Bf 109 (straight wing) aircraft in 1938 by its designer, Wolfgang Liebe [1]. There was a robust secondary flow (spanwise flow) from the root to the tip of the wing when the stall started in this aircraft. Applying a wing barrier stopped this cross flow, which in turn reduced stall difficulties. Lift distribution is changed and the tip lift load is reduced by wing fence. In most cases, a swept rearward wing and a straight wing with a high angle of attack will benefit more from wing fencing [2]. A wing's free stream velocity becomes a normal and tangential component to the leading edge as it sweeps rearward.

Because of the geometry of sweptback wings, the aft end of any aircraft will always be after the CG. Therefore, a pitching moment (nose down) is created by lift at the wing tip. There will be a quick decrease in lift and nose-down pitching moment if the wingtip stalls. A trimmed airplane will experience a nose-up pitching moment as a result. As a result of this instant of nose-up pitching, the angle of attack increases and the wing stalls along most of its length. An abrupt and powerful pitch-up and subsequent full stall are the outcomes. Recuperating from this is quite challenging for pilots. The use of wing walls may help postpone or eradicate this issue.

International Journal of Engineering Research & Technology (IJERT)
ISSN: 2278-0181
Vol. 15 Issue 07 , July - 2026

Typically, it extends to a length equal to one-third of the chord, including the majority of the region responsible for producing lift. If you want the best outcomes, you should make sure that the fence is taller than the border layer. It will be far more beneficial to place fences at the 1/3 and 2/3 locations along the length of the semi-span. The wing fence is a kind of prospective fence, boundary layer fence, or boundary fence. Actually, wing fences also include winglets and engine pylons.

Using a half-aircraft model with a simple/extended fence, Solfelt D.A. conducted computational research on the T-38 Talon's wing fence effects. He claims that at a 15° angle of attack, the coefficient of lift (CL) increases by 4.9% with an expanded barrier.

2.4 Objectives

Applying wing fences improves lift production, reduces induced drag, and improves stall characteristics by reducing the generated secondary flow (Spanwise flow) of a swept backward wing, which is the major aim of this computer work. Studying on the Grid Alone To get the most accurate and suitable findings in computational fluid dynamics (CFD) analysis, grid independence examination is needed. Figure 3 shows the fluid domain that is used for the grid independence investigation. In this domain, C represents the length of the root chord (Cr). The dimensions of the models are taken from Table 1. The computational analysis is carried out using the GAMBIT and FLUENT software packages.

S.No	Description	Dimension
1.	Aerofoil Type	TSAGI 12%
2.	Wing Type	Straight Wing
3.	Root Chord Length (C_r)	2 m
4.	Tip Chord Length (C_t)	1.5 m
5.	Wingspan Length (b)	5m
6.	Leading edge Sweep Angle (Λ_{LE})	0
7.	Aspect Ratio (AR)	2.5

Table 4 : Geometric specifications for the wing

The domain of fluids makes use of pressure far fields, symmetry, and boundary conditions on walls.

Mesh Type	Number of Cells	Minimum Volume (m^3)	Maximum Volume (m^3)	C_L
A.	1,62,684	$7.74*10^{-7}$	$3.27*10^{-1}$	0.050302304
B.	2,78,653	$6.98*10^{-8}$	$3.73*10^{-1}$	0.047456289
C.	3,76,851	$9.75*10^{-8}$	$3.79*10^{-1}$	0.047402813
D.	5,85,788	$8.97*10^{-8}$	$3.19*10^{-1}$	0.046251209
E.	6,92,574	$1.29*10^{-8}$	$3.42*10^{-1}$	0.0451604
F.	7,87,464	$7.60*10^{-9}$	$3.27*10^{-1}$	0.04509114

Table 5: Mesh independece study comparing grid densities

The CL value for mesh types E and F is about the same, according to the table's results. The time and memory needed for the numerical simulations are taken into account when selecting mesh type 'E' for the subsequent simulations. Simulating and integrating In GAMBIT, models are designed according to the dimensions for the simulation.

For the CFD, these models have mesh-type 'E.'

International Journal of Engineering Research & Technology (IJERT)
ISSN: 2278-0181
Vol. 15 Issue 07 , July - 2026

Model Number	Fence Nature	Fence Location from the Root	Lying Surface	Fence Height
1.	Without fence	Not Applicable	Not Applicable	Not Applicable
2.	Single Fence	At 50% of span length	On Upper Surface	5cm (2.5% of Cr)
3.	Double Fence	At 30% & 60% of span length		
4.	Single Fence	At 70% of span length		
5.	Single Fence	At wingtip		
6.	Single Fence	At 50% of span length	On Lower Surface	
7.	Double Fence	At 30% & 60% of span length		
8.	Single Fence	At 70% of span length		
9.	Single Fence	At wingtip		
10.	Single Fence	At 50% of span length	On Upper Surface	15cm (7.5% of Cr)
11.	Double Fence	At 30% & 60% of span length		
12.	Single Fence	At 70% of span length		
13.	Single Fence	At wingtip		
14.	Single Fence	At 50% of span length	On Lower Surface	
15.	Double Fence	At 30% & 60% of span length		
7.	Single Fence	At 70% of span length		
1.	Single Fence	At wingtip		

Table 6: Fence configuration summary

2.5 Results Of The Analysis

The stall angle of attack is often the sweet spot for the produced secondary flow. Therefore, the wing models that were constructed with a 45-degree sweep angle are examined at an angle of attack of 10 degrees (M=0.6). A measure of aerodynamic efficiency, CL/CD, is derived from the computational analysis of the lift coefficient (CL) and the drag coefficient (CD).

	C_L	C_D	C_L/C_D
Wing without fence	0.53350604	0.048482771	11.0040335

Table 7: At α = 10°, the outcomes of a 45° swept rearward wing missing a fence

	Fence Nature	Fence Location from the Root	C_L	C_D	C_L/C_D
On Upper Surface	Single Fence	0.5b	0.57233016	0.045903758	12.47
	Double Fence	0.3b & 0.6b	0.57323572	0.046878863	12.23
	Single Fence	0.7b	0.58385903	0.043904005	13.30
	Single Fence	b	0.57155353	0.045533606	12.55
On Lower Surface	Single Fence	0.5b	0.53992388	0.048369757	11.16
	Double Fence	0.3b and 0.6b	0.54304456	0.048981517	11.09
	Single Fence	0.7b	0.53721863	0.047684166	11.27
	Single Fence	b	0.55788077	0.046374649	12.03

Table 8: The outcome of a 45° swept rearward wing with a 5cm height barrier at an angle of 10°

International Journal of Engineering Research & Technology (IJERT)
ISSN: 2278-0181
Vol. 15 Issue 07 , July - 2026

	Fence Nature	Fence Location from the Root	C_L	C_D	C_L/C_D
On Upper Surface	Single Fence	0.5b	0.57622394	0.048015872	12.00
	Double Fence	0.3b and 0.6b	0.57605677	0.052712929	10.93
	Single Fence	0.7b	0.5736185	0.051018766	11.24
	Single Fence	b	0.56310159	0.04673919	12.05
On Lower Surface	Single Fence	0.5b	0.54485159	0.04805102	11.34
	Double Fence	0.3b and 0.6b	0.54886673	0.048903298	11.22
	Single Fence	0.7b	0.53432774	0.048188528	11.09
	Single Fence	b	0.57721698	0.046587315	12.39

Table 9: Conclusions drawn from a 45° swept rearward wing with a 15cm height fence operating at α = 10°

Angles Swept Backward in Relation to a 15-centimeter-High Fence at Natural Site CL 0.5b 0.57622394 Fence 0.3b and 0.6b 0.57605677 0.7b 0.5736185 b 0.56310159 0.5b 0.54485159 In the context of a 5cm and 15cm fence, the fluctuation in CL and CD is shown by Double Fence 0.3b and 0.6b 0.54886673 0.7b 0.53432774 b 0.57721698. It is evident that the root of C is at 5 cm for the fence height (hf). Additionally, CD is at its lowest in that area. The results suggest that a fence with a height of 15 cm is not as effective as a surface-located CL and CD variation (Vadivelu, P., Lakshmanan, D., & Rajasekar, S.). K. Prasad and G. NAAS Rating: 3.11 0.048981517 11.09 0.047684166 11.27 0.046374649 12.03 Swept Backward Wing with 15cm It can be shown that CL is at its highest when the height of the fence is at its lowest, with the following values: 12.00 0.052712929 10.93 0.051018766 11.24 0.04673919 12.05 0.04805102 11.34 0.048903298 11.22 0.048188528 11.09 0.046587315 12.39. Therefore, with hf=5 cm, we get an increase in CL/CD at effective as a fence.

For fences that are 5 cm and 15 cm high, the wing's C also varies. For h at the wing tip. Additionally, at points C 9 and 10, it suggests that barrier with a wing. Optimization of Spanwise Flow Reduction by Lower Surface Estimation with the Use of Wing Fence For fence heights of 5 cm and 15 cm, the SCOPUS Indexed Journal Surface - CL/Cd Variation with Respect to Fence placement shows how CL and CD vary with respect to the wing's placement. At hf=15 cm, the C tip is plainly visible. Additionally, CD is at its lowest in that area. The outcome is an enhanced CL/CD ratio, albeit a fence with a height of 5 cm is not nearly as effective as one with a height of 15 cm on the surface. This information is sourced from 1637, editor@tjprc.org. From the ground level, it is easy to see that CL is at its highest for fence D, which is the tip fence, regardless of its location or height. The bottom surface measures 15 cm, as seen in the figure.

It is noted that there is secondary flow around the bottom surface tip from the Z velocity contours of all the examples. Likewise, the very top of the surface. Journal Impact Factor (JCC): 7.6197 SCOPUS Indexed Surface - CL/CDVariation with Respect to Fence is written by Vadivelu. P, Lakshmanan. D, Rajasekar. K, and Prasad. G. Case A) without a fence has a location velocity component variation of 5 cm at 0.7 b on the top surface, while Case C) with a fence has a location velocity component variation of 15 cm at the lower surface tip. Across all examples, the use of fences on secondary flow is noticeable. Similarly, the secondary flow at Vadivelu is reduced by using barriers on lower surfaces. P. Lakshmanan and D. Rajasekar are the main authors. K & Prasad. G. NAAS Rating: 3.11 Fence Position and Height for Cases A) Absent a fence, with a height of 15 cm at the top of the lower surface, decreases

The results of the computational fluid dynamics (CFD) study confirm that fences may improve the wing's performance by decreasing generated drag. A fence that is 2.5% of the root chord's height is effective on the top surface of this simulation, while a fence that is 7.5% of the root chord's height is effective on the bottom surface. In particular, at the 0.7b spot on the top surface, a fence with hf=5cm works well, and at the wing tip on the bottom surface, a fence with hf=10 works well. Use of both of them together should result in a significant improvement in the wing's performance. It has been determined from the study and prior research that there is no optimal wing fence position or dimension. The wing's geometry and free stream condition determine the difference.

The object in question may be referred to by a number of names, including "wing fence," "boundary layer fence," "potential fence," or even just "fence." For the last half-century, swept-wing aircraft have made use of wing barriers. One of the first aircraft to employ them was the MiG-15, which had two fences per wing. They were also used by the F-86. Modern aircraft, such as the Fiat G 91 and the Hawk and Harrier from BAe Systems, also use fences. Even while wing fences are often associated with supersonic and near-supersonic planes, they may be useful for low-speed swept-wing aircraft like RC models and man-carrying sailplanes. Within those domains, examples include the Akaflieg Braunschweig SB-13 and a version of CO8 by Hans-Jürgen Unverferth by Glyn Fonteneau and Dave Camp. Wing fences are fascinating for their history and the impact they may make. A wing fence is only a flat plate

International Journal of Engineering Research & Technology (IJERT)
ISSN: 2278-0181
Vol. 15 Issue 07 , July - 2026

fastened to the wing at an angle that allows air to flow freely past it. While working on the Messerschmitt Bf 109B, Wolfgang Liebe is said to have invented the device; in 1938, he was granted a patent in Germany for it. There was something unusual about the Messerschmitt Bf 109B's stall. A stall began at the base of the wing and quickly spread out toward the leading edge, creating a cross-span flow. Because of this aerodynamic behavior, the wing stopped all at once, which is a very hazardous trait. The stall issue was resolved by the installation of a wing barrier, which blocked the flow over the bridge. The fact that the Bf 109B's solid plate blocked the passage of cross span at the wing surface may seem apparent. But the real secret was that the barrier created a vortex when you started a sideslip, which was the concealed mechanism that really worked. The function of wing fences on swept wings is very different from that on a straight wing, like the Bf 109B, yet they are helpful in limiting the ugly stall behaviors that come with extreme sweep angles. Wing fences have been known by different names, as we noted in the first parenthetical paragraph. The most popular one is "boundary layer fence," therefore let's examine it closely. The area immediately around a solid object's surface when the overall pressure drops significantly is called the boundary layer. To rephrase, the speed represents a percentage of the free-stream flow. It is common practice to measure the distance perpendicular to the surface at which the velocities reach 99% of the main flow's value to determine the boundary layer thickness. In actuality, the boundary layer is often only a few millimeters thick, even on full-size planes. Bear in mind the above definition:

Building a wing fence to match the thickness of the boundary layer renders it ineffective. Actually, fences need to be rather tall to be effective. • Since the boundary layer thickens as one approaches the wing's trailing edge, the fence, if its height were determined by this property, would be set at its highest point near the wing's trailing edge. However, a fence's efficiency is unaffected by its length being far longer than 50% chord. • A wing fence, when wrapped around the front edge, is usually more effective. All of the foregoing prove that "boundary layer fence" is an inaccurate description. Wing fences influence the potential flow—a flow in which the vorticity is zero—in a way that has an indirect effect on the boundary layer. What the fence does to the potential flow is where the name "potential fence" comes from. We will do our best to simplify the key ideas, but wing fences on swept wings are very complicated and their operation is still a mystery. Think of a wind tunnel setup with a swept wing panel and the lift distribution that goes along with it. It should be noted that the wing panel of a swept back wing is obtained by removing the right wall, while the wing panel of a swept forward wing is obtained by removing the left wall. cl y air movement Wind tunnel diagram showing sweeping wing and the distribution of lift it generates. Removing the walls and connecting a "mirror" wing panel to the left or right end of the current wing creates a whole wing that can be swept forward or backward, and the corresponding lift distribution is shown in, from a slightly different angle. A wing fence is similar to a tunnel wall from an aerodynamics perspective. A more thorough demonstration of this phenomenon is provided. As shown in Figure 4, the distribution of lift on a swept back wing may be altered by installing a wing barrier. Be careful to observe that c l is greater on the inside of the fence and lower on the outside. Because the weight is now on the inside of the fence, stall behavior is much improved. Around forty percent of the semi-span from the base of the wing should be where the climax should be placed. This section of the wing should stall when the angle of attack is high, allowing the root and tip of the wing to keep lifting and causing a little pitch down moment. Separate flow due to high attack angles fundamentally involves the boundary layer. In order to restrict or regulate flow separation, corrective procedures must impact the boundary layer. The border layer is unaffected by wing barriers, as mentioned above. Instead, they affect the boundary layer by influencing the potential flow. Overall, the boundary layer is maintained in a manner that allows separation, and the overall stress on the wing tips is minimized. The distributions of lift and swept wing segments are related concepts. restrained, and the tendency to stall is ameliorated.

Wing fences seldom go beyond one-third of the wing chord. The chord's most elevated region is the front third. The sweep effect and the "mirror" idea, shown in Figures 1 through 4, likewise work well in this region. It is common practice to use sturdy paper or plastic to build RC sailplane wing fences with a profile like the ones shown in Figure 5. You can easily remove, change, or experiment with them since they may be connected using tape. Fencing the area between the wing's leading edge and its trailing edge is the standard practice. Figure 3 shows that airflow is cl y A B A' B' A-A' B-B' at a spot just in front of the inner edge of the aileron or elevon. "Mirror" swept wings and the lift distributions that go along with them.

Total swept wing design with right wing fence and lift distributions used. shown to be very helpful in reducing undesirable stall behaviors while keeping the control surface functional at high attack angles. On wings with a high aspect ratio and steep sweep angles, it has been discovered that installing two fences on each panel, at 1/3 and 2/3 of the semi-span, is productive. Wing fences might be difficult to see at times. Below the wing, on pylons, are often located the engines of most airplanes. In addition to the pylon itself acting as a lower-surface fence, the leading-edge pylon fairing often extends over the leading-edge to provide an upper-surface fence. Many methods exist for improving the flying characteristics of swept wings by controlling the airflow. Some examples are wing slots, which were discussed in our column from August 1994, leading edge slats, and the so-called "saw tooth" leading edge.

International Journal of Engineering Research & Technology (IJERT)
ISSN: 2278-0181
Vol. 15 Issue 07 , July - 2026

However, wing fences are appealing due to their ease of fabrication, attachment, and modification, all of which do not impact the primary airframe in any kind. Their approach is the most suitable in terms of cost and the opportunity to explore.

Aircraft wings may be equipped with permanent aerodynamic devices called wing fences, boundary layer fences, or potential fences. Wing fences, which commonly encircle the leading edge of swept-wing aircraft, are flat plates fastened to the top surfaces of the wings in a parallelogram pattern with the chord of the wings and perpendicular to the direction of free stream airflow. In contrast to wingtip devices, which aim to recover vortex energy in order to boost aerodynamic efficiency, these devices prevent the whole wing from stalling simultaneously by impeding span-wise airflow down the wing.

A swept-wing aircraft's leading edge angle directs a portion of the airflow to the wing tip when the aircraft approaches the stall speed of the wing. This is an iterative process, as the leading edge angle and the spanwise airflow from the wing root both influence the airflow close to the wing's center. The effective airspeed declines significantly below the stall when the airflow is almost entirely spanwise at the wing tip rather than front-to-back across the wing. Lift created at the wingtips tends to induce a nose-down pitching moment because the geometry of swept wings usually positions the wingtips of an aircraft behind its center of gravity. The lift and the nose-down pitching moment are both quickly reduced when the wingtips stall. Once the nose-down pitching moment is gone, the aircraft becomes unbalanced and has a net pitching moment that is up. Stall across a larger section of the wing occurs as a result of the aircraft's nose being forced upward, which increases the angle of attack. The end effect is a hard stall after a quick and strong pitch-up, from which the pilot has a tough time recovering.[1] Notable instances of this behavior include the "Sabre dance" (which led to the crashes of several F-100 Super Sabres).

The spanwise flow can't go too far down the wing and become too fast, therefore wing gates stop it or at least slow it down. Redirecting the airflow over the wing surface occurs when the plane encounters the fence. Avro Arrow-style notch or dogtooth leading edge detailing or slats used in previous F-86 iterations were two examples of comparable solutions. Not only may the slats' actuators serve as gates, but they can also improve the wing's angle of attack response and decrease the stall speed, thereby reducing the issue.

Despite the fact that wing barriers had been known in the UK since 1914, the invention is often credited to Liebe of Messerschmitt, a German aerodynamicist, who filed a patent application in 1938.

With the advent of subsonic swept wings in 1947, the United States and the Soviet Union separately deployed the Lavochkin La-160, Mikoyan MiG-15, Northrop YB-49, and McDonnell XF-85. From the MiG-15 to the MiG-25, the RAF's spin research program (which started in 1912), the creation of the Tu-128 to the Tu-160, and the Su-7 to the Su-22 were all examples of the Soviet Union's extensive and lengthy usage of such barriers.

Wing fences aren't quite as good as wingtip devices when it comes to reducing induced drag; they work by raising the lifting system higher.

Originally developed for use in military activities, small radio frequency-controlled aircraft eliminate the dangers associated with human vehicles. These flying wings-shaped unmanned aerial vehicles (UAVs) came up as a practical and economical substitute for human pilots, allowing missions to be carried out without the risks associated with human flight. Their civilian uses have grown over the years to include monitoring the environment, collecting data on weather patterns, aerial mapping, precision agriculture, and logistics. This change exemplifies how flying-wing designs may adapt to various tasks and flight limitations. Aerodynamic efficiency and stability are greatly affected by the choice of airfoil in this scenario. Airfoils are essential to all types of aerodynamic platforms, including gliders, micro UAVs, and commercial aircraft. The cruising speed, Reynolds number, payload, and desired level of flying autonomy are mission-related considerations when selecting an airfoil. In the case of flying wings, especially, without a traditional tailplane, aerodynamic loads become more sensitive; hence, the airfoils should have a high lift coefficient at moderate angles of attack 5 to provide a stable pitch and roll.

The lift and drag coefficients are the main features of the aerodynamic performance of an airfoil. The lift-to-drag efficiency is their ratio and is an important indicator of aircraft aerodynamic optimization. To achieve a high, it is necessary to achieve maximum lift without causing too much viscous or pressure drag which directly relates to the endurance and energy consumption. To enhance contemporary aerodynamic design computational fluid dynamics (CFD) is now a key instrument in the estimation of these parameters as well as guiding optimization.

International Journal of Engineering Research & Technology (IJERT)
ISSN: 2278-0181
Vol. 15 Issue 07 , July - 2026

New computational optimization and artificial intelligence techniques have greatly enhanced the design of airfoils. Vinuesa et al. used deep reinforcement learning to control active flow in the wings with low aspect ratio, and Robb and Paul used spanload optimization to enhance the flying-wing stability. Likewise, Lianetal. surveyed the advances of evolutionary algorithms to aerodynamic design and later research has (considered multi-objective approaches and learning-based surrogates under low-Reynolds conditions). These works indicate a paradigm shift of hybrid methods that is the core of the knowledge of aerodynamic and structural coupling effects that rule the stability of small-scale UAVs. This paper will outline the design, numerical model, construction, and flight test of a delta-wing UAV that has been optimized in the atmo spheric conditions of Bogota, Colombia which is characterized by high altitude (around 2550 m) and low air density. The workflow will include (i) aerodynamic profile selection and CFD evaluation under local con conditions, (ii) a sequence of fuselage and wing-fence integration and subsequent improvement of the static and dynamic stability and (iii) experimental validation through IMU-based telemetry and statistical analysis of the flight performance. This multidisciplinary project will also seek to offer a convenient, data-driven process of the aerodynamic design of low-cost UAVs flying within low-Reynolds conditions. 2. Methods 2.1. Overview and workflow The methodological workflow followed in this research is summarized It comprises four main stages: (i) airfoil screening and aerodynamic analysis, (ii) parametric design of the fuselage and integration of electronic components, (iii) CFD-based evaluation of passive f low devices (winglets and fences), and (iv) manufacturing and experimental validation through repeated flight tests. This structure not only guarantees computational consistency, but also experimental reproducibility

Uniqueness In flying wings, there are no horizontal stabilizers and this poses unique aerodynamic challenges. They can be prone to pitch oscillations, and lateral instability caused by their highly swept geometries and center-of-pressure variability.Winglets and wing fences are commonly used to counter the effects of these by using passive control surfaces. Winglet vertical extensions on the wingtips-induced drag-are reduced by alleviating wing tip vortices. Wing fences (or flow correctors), illustrated in the figure, are flat surfaces that are vertically aligned over the span to restrict the migration of spanwise flow, delay separation of the boundary-layer, and improve longitudinal and lateral stability. Recent studies-including experimental/para metric studies as well as large-eddy level simulation studies-have indicated enhancement of post-stall performance, drag and effective damping in delta wing UAVs with fences installed . Delta-wing designs, common in UAVs and micro air vehicles are based on special airfoils that can hold attached f low at high angles of attack. Profiles like WORTMANN FX 63-137 and A18 give preferable pressure gradients which postpone flow separation and profiles like Clark Y, DF101 and MH45 utilize camber modulation to strike equilibrium between lift and static stability. To choose an optimal profile one must then trade off aerodynamic efficiency and manufacturability and stability in a desired Reynolds range [6,7,18]. Structurally, the choice of the lightweight and re silient materials is also critical. Despite the ever growing popularity of carbon composites, polystyrene and balsa wood are still used in experimental and educational UAVs due to their low prices, ability to shape, and desirable strength-weight ratio. However, these materials would need to be reinforced-usually by spars or composite mesh-to allow them to withstand bending and torsional loads in dynamic operations [19-22]. The combination of aerodynamic optimization and structural design facilitates low cost but robust solutions that can be easily verified using an experiment. Even though there has been much development on CFD and optimization methods, few studies have been done to experimentally verify the aero dynamic stability enhancement mechanism of flying-wing UAVs in low density, high altitude environments. Moreover, not many works combine numerical optimization, passive control devices (wing fences), and works in the real world based on validation through telemetry. Filling these gaps is a core issue to the aerodynamic and structural coupling effects which determine stability in the small-scale UAVs.

This project shows the design, numerical modeling, manufacturing, and flight test of a delta-wing UAV that is optimized to the conditions of the atmo sphere Bogota, Colombia-high-altitude (about 2550 m) and low air density. The workflow includes (i) aero dynamic profile identification and CFD based analysis under local conditions, (ii) progressive fuselage and wing-end integration to stimulate both static and dynamic stability, and (iii) experimental validation of the work by IMU-based telemetry and statistical analysis of flight performance. The objective of this multidisciplinary methodology is to offer a convenient and data-driven framework to the aerodynamic design of low-cost UAVs that are to operate in low-Reynolds flows. 2. Methods 2.1. Overview and workflow The methodology workflow of the research is summarized in Fig. 4. It consists of four key phases: (i) screening and aerodynamic analysis of the airfoil, (ii) parametric design of the fuselage and electronic components assembly, (iii) evaluation of passive f low devices (winglets and fences) with the help of CFD, and (iv) manufacturing and experimental verification using repeated flight tests. This architecture guarantees computational consistency as well as reproducibility of experiments.

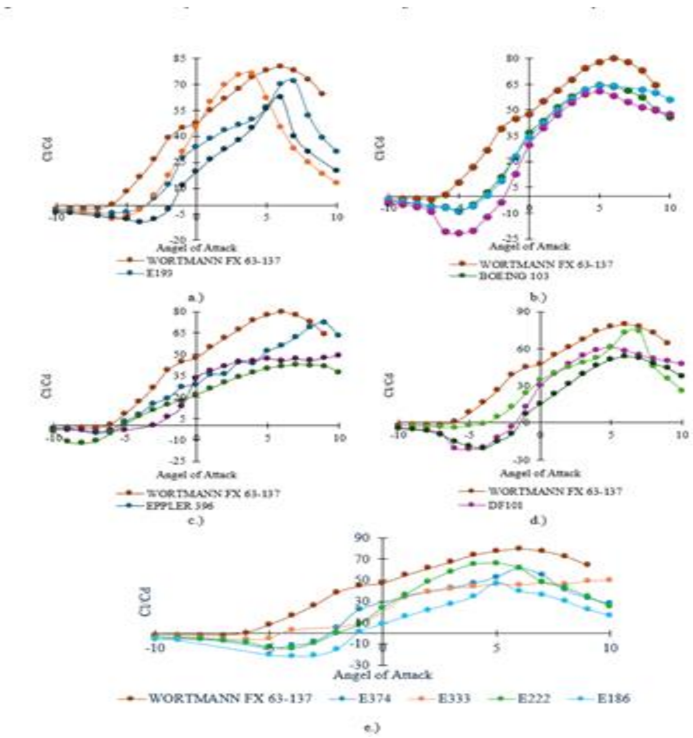

Graph 4 : Aerodynamic performance date for different wing profiles

Evaluation and choice of airfoils To guarantee a comprehensive coverage of thickness-to-chord ratios, camber lines, and Reynolds number flexibility throughout the range of 1.4 × 105-7.4 × 105, twenty representative airfoils from the Wortmann, Eppler, Clark, and Boeing families were originally analyzed using XFLR5. Despite initial expectations that the Wortmann family would do well at low Reynolds numbers, the inclusion of the more comprehensive set was done to **avoid bias** and **confirm the selection by comparative aerodynamic evidence** instead of preconceptions. The lift-to-drag ratio ($\mathbf{OO}/\mathbf{O}D$) and pitching-moment stability ($\mathbf{O}M$) were the screening criteria. The first collection of geometries includes Wortmann, Eppler, Clark, and Boeing geometries encompassing thickness/camber variations throughout □$e \in [1.4, 7.4] \times 105$ in order to prevent prior-family bias and to encourage selection based on comparative evidence instead of expectation. The selection was done using $E = \mathbf{OO}/\mathbf{O}D$ and a negative and steep enough $d\mathbf{O}m/d\beta$. Section 2.3 deals with the design and integration. An aircraft wing was created using the selected airfoil (EPPLER 396), which was parametrically designed in SolidWorks. In order to achieve the lowest feasible drag while maintaining the maximum interior capacity and a center of gravity that does not exceed 2025 percent of the mean aerodynamic chord, a number of fuselage designs were designed. A 3DR Pixhawk inertial measurement unit (IMU) was included into the design to track variables such as airspeed, height, yaw, roll, and pitch. The predicted aerodynamic stability was validated using these data, which were recorded by the on-board telemetry system. 2.4. Fluid dynamics (FFD) modeling of flow control devicesThe researchers used ANSYS Fluent 2024 R2 to do numerical simulations in both steady-state and transient scenarios. At low Reynolds numbers, the realizable 0 -epsilon model was used to represent turbulent dissipation. When the aerodynamic coefficients stabilized within 1% and the convergence conditions were met (residual decreased below 10-5), the mesh-independence was established using the three stages of refinement (0.6-1.5 million elements). We used the standard NACA criteria for induced-drag reduction to guide the parametric introduction of wingslets and barriers. Optimizing their shape, they were able to reduce generated drag and improve pitching stability by deflecting the tip vortex core 10-12% spanwise.

The near similarity of CFD predictions and telemetry measurements confirms the credibility of the proposed workflow to low-cost UAV applications in high-altitude, low-density settings. 4. Conclusions This paper designed, simulated and experimentally tested a delta-wing UAV with passive flow-control devices to operate in the high-altitude environment of Bogota. The EPPLER 396 airfoil was determined by the aerody namic evaluation to offer the best profile to achieve high efficiency (71.2), and the target Reynolds range that would lead to a stable pitching moment behavior (0.045). The wing fences-winglet combination successfully reduced the separation of spanwise flows with a 8 percent reduction in induced drag as well as a 32 percent enhancement in roll damping compared to the baseline design. These numerical predictations were confirmed by the telemetry based flight analysis, longitudinal damping ratios averaged at 0.36 and roll oscillations were limited to +-4 degrees.

International Journal of Engineering Research & Technology (IJERT)
ISSN: 2278-0181
Vol. 15 Issue 07 , July - 2026

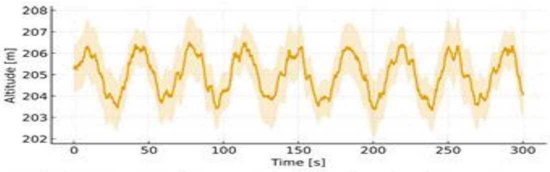

Fig. 17. Altitude over 300 s: Climb, capture of level flight, and steady regulation around 205 m.

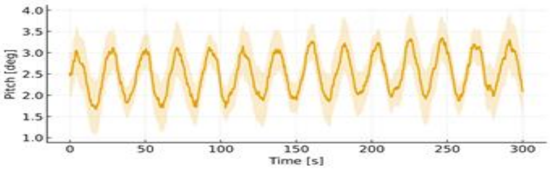

Fig. 18. Pitch time history: Exponential decay toward trim, $\zeta_1 \approx 0.36$.

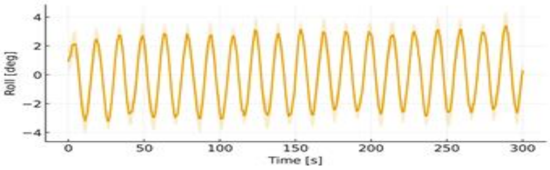

Fig. 19. Roll dynamics during loiter: Bounded dispersion and increased damping relative to baseline.

Graph 5: Roll dynamics during loiter

The quantitative results indicate the stability of the suggested arrangement dynamically. The near similarity of the simulation and experimental results confirms the adopted CFD-IMU workflow as a solid methodology of conducting research on low Reynolds UAV. The prototype made of polystyrene and balsa wood structurally met the desired stiffness-to-weight ratio and could be loaded with several flights and insignificant impacts without any deformation, suggesting that producing cost-effective prototypes is possible. The design, although made to match the conditions of Bogota did not disprove that it would perform well in flight in Bucaramanga, thus validating the adaptability to different atmospheric densities. This framework should be expanded with the future work by adding composite materials, advanced aerodynamic optimization, and flow visualization techniques to capture the unsteady vortexes dynamics.

The suggested approach is a tried and true manner for tiny UAVs to be co-designed with their structures for low-density, high-altitude missions. Honesty and transparency There is no perceived conflict of interest between the writers and the publishing of their work. No particular grant from any governmental, commercial, or non-profit organization supported this study. Written work by J.A. Parada-Marin (review and editing), Ricardo Alfonso Jaimes Rolon (validation), O. Bohórquez (conceptualization), and software, resources, project administration, methodology, investigation, formal analysis, data curation, and supervision are all part of the CRediT authorship contribution statement. Subjects covered by Wilman-Alonso Pineda-Muñoz include writing (review and editing), writing (original draft), visualization, methodology, and investigation. Work history: Saul-Andrés Hernández-Moreno: Writing, reviewing, and editing; work history: original draught; supervision; methodology; funding acquisition; validation; investigation; and work history: original draught. Requests for data will be promptly addressed. Conflict of interest disclosure The writers of this article affirm that they are free from any ties or financial conflicts of interest that may have seemed to impact their work.

CHAPTER 3

METHODOLOGY

The primary use of ANSYS is to replace physical testing. Instead of building ten differential wings and breaking them to see which is strongest, an engineer builds one digital model and tests it under thousands of virtual conditions.

- **Crash Simulation:** Simulating the deformation of a vehicle structure in case of an impact to safeguard the passengers.
- **Fatigue Analysis:** The calculation of the number of thousands of rotations that a turbine blade can make, until a microscopic crack develops.

- **Fluid Dynamics and Thermodynamics.**
- Users of ANSYS Fluent or CFX simulate the behavior of liquids and gases that have surfaces.
- **Aerodynamics:** The art of streamlining a car or an airplane to minimize the drag and to enhance fuel efficiency.
- **cooling:** Developing coolers in high-performance computers or coolers in electric vehicles (EVs).
- **Electromagnetic & Antenna Design**
- ANSYS is applied to make sure that devices are able to communicate with the emergence of the IoT and 5G without interference.
- **Signal Integrity:** The high-speed data on a circuit board is to be made sure that it is not corrupted by other components surrounding it.
- **Electric Motors:** To optimize the magnetic fields in EV motors to make them have a longer range and provide more torque.
- **ANSYS in the Contemporary Industry.**

ANSYS scope is characterized by Multiphysics capability, which is the capability of modeling the interaction of various physical forces at the same time.

A.Aerospace and Defens

This is the most crucial of ANSYS scopes. It is applied to model supersonic flight, cabin pressurization and engine combustion. The software assists in achieving high FAA/EASA safety approvals even before a plane takes off the ground.

B.Automotive Industry

The focus here has been very much shifted to the Autonomous Vehicles (AVs) and Electrification. ANSYS is applied to model radar/lidar sensors and train AI drivers in a virtual environment and the complex chemistry and thermal runaway hazards in lithium-ion batteries.

C.Biomedical Engineering

ANSYS is used to design life-saving medical devices.

Stents & Implants: Simulation Of a heart stent in an artery.

Orthopedics: Evaluating the lifespan of artificial knee or hip joints depending on particular bone density of a patient.

D.Civil & Structural Engineering

The program is applied to examine the "Health" of the large-scale infrastructure.

Seismic Analysis: The representation of the motion of a skyscraper or bridge in case oan earthquake.

Wind Loading: Experimenting on the interactions of the speeding winds on tall buildings glass facades.

3.Future Perspective Digital Twins and AI.

ANSYS is now expanding its scope to Digital Twins. This is done by developing a virtual simulation of a physical object (such as a jet engine) that is already operational.

The model in ANSYS is fed with data provided by sensors on the actual engine in real-time.

It has software which just knows when a component will malfunction before it does, which makes it possible to do Predictive Maintenance.

International Journal of Engineering Research & Technology (IJERT)
ISSN: 2278-0181
Vol. 15 Issue 07 , July - 2026

3.1 ANSYS Fluent

ANSYS Fluent is a design and analysis program of computational fluid dynamics (CFD) software widely used in fluid flow systems. Being a strong part of the ANSYS simulation software package, it plays an essential role in solving complex fluid flow problems in various industries, such as aerospace, automotive, chemical and energy. As a powerful tool to solve the governing equations of the fluid dynamics, namely the Navier-Stokes equations, ANSYS Fluent effectively employs the use of numerical techniques, including finite volume methods. Complex flow simulations such as laminar and turbulent flow, multi phases flow and reacting flows can be widely configured and executed by engineers. The software has very sophisticated features, such as analysis of heat transfer, turblulence modelling, and tracking conditions of the particles. In addition, it also provides a variety of boundary conditions such as inlets, outlets, walls and symmetry planes and the choice of post-processing and display of the results of the simulation. ANSYS Fluent can be used to perform parallel processing, allowing its users to run simulations on high-performance computing clusters. Moreover, it has proper customization capabilities, allowing the user to create their own custom models and functions, depending on their needs. ANSYS Fluent is a complete CFD software package with its versatility and power, providing a complete solution to fluid flow analysis. Its ability to deal with the wide range of fluid flow issues, easy to use interface, and extra features have enabled it to become popular amongst engineers and researchers in many industries. ANSYS Fluent is developed to be easy-to-use, simplifying the set-up, running and analysis of CFD simulations and with numerous mesh conditions.

3.2 The Functional Scope of Fluent.

Technical coverage Fluent is capable of dealing with complex physics not possible with other simpler tools:

Incompressible and Compressible Flow: Low-speed water pipes to high-Mach number aerospace confusing (as in your previous airfoil pictures).

Heat Transfer: Modeling conduction, convection, and radiation. This plays a vital role in cooling engine and electronics thermal control.

Multiphase Flow: The interaction between alternate phases of matter, such as air bubbles in oil, droplets in a spray or boiling liquids is simulated.

Chemical Reaction/Combustion: Simulating the burning of fuel in a gas turbine or an internal combustion engine, as well as pollutant emissions, such as NOx and SOx.

Dynamic / Moving Mesh: This capability allows parts of a calculation to move, like a wind turbine rotating or a piston in a cylinder.

Industrial Scope: Fluent Usage.

- **Aerospace and Defense**

The industry leader in the field of external aerodynamics is Fluent. Its scope includes:

High-Alpha Flight: Control of wings (stall and separation) by means of fences or slats.

Spacecraft Re-entry: Simulating the high temperatures and pressure in the atmosphere

when a capsule re-enters it.

Propulsion: The internal flow of jet engines and rocket nozzles.

- **Automotive Engineering**

The focus has now been transferred to aerodynamics as it was in the past, but to the so-called Green Revolution:

Battery Safety: Thermal Runaway (EV battery) simulation to prevent fires.

HVAC Systems: streamlining air conditioning circulation in a car cabin with comfort in mind.

International Journal of Engineering Research & Technology (IJERT)
ISSN: 2278-0181
Vol. 15 Issue 07 , July - 2026

External Aero: How to make the electric cars have a longer range by minimizing their drag coefficient (USD CdUSD).

- **ENERGY and POWER.**

Renewables: Making the offshore wind turbine massive and optimal through maximizing the blade pitch.

Nuclear & Oil/Gas: Simulating cooling cycles in nuclear reactors or the flow of crude oil through thousands of miles of subsea pipelines.

- **Healthcare and Life Sciences**

Respiratory Studies: Modeling how medicine from an inhaler travels through the human lungs.

Blood Flow: Simulating how blood moves through artificial heart valves to prevent clotting.

- **Research and Academic Scope**

In the academic world, Fluent provides a platform for **Verification and Validation**

New Turbulence Models: Researchers use Fluent to test new mathematical theories for turbulence (like LES or DES) against experimental wind tunnel data.

Optimization Algorithms: Using Fluent's "Adjoint Solver," which automatically suggests the "perfect shape" for an object to minimize drag or maximize cooling.

- **Summary: The Breadth of Fluent**

The "Scope" of ANSYS Fluent is essentially **anything that involves a fluid.** If an engineer needs to know the pressure, temperature, or velocity of a gas or liquid at any

3.3 Transition SST (4 Equation) - γ-Re$_\theta$ model

The Navier-Stokes Equation is the primary tool for Ansys Fluent in finding a solution to the issue.

$$\frac{\partial \rho}{\partial t} + \frac{\partial}{\partial x_j}(\rho U_j) = 0 \qquad (3.1)$$

$$\frac{\partial}{\partial t}(\rho U_i) + \frac{\partial}{\partial x_j}(\rho U_j U_i) = -\frac{\partial p}{\partial x_i} + \frac{\partial}{\partial x_j}\left[\mu_{eff}\left(\frac{\partial U_i}{\partial x_j} + \frac{\partial U_j}{\partial x_i}\right)\right] \qquad (3.2)$$

To discretize these equations, a finite element approach based on control volumes is used. To achieve both first- and second-order precision, the spatial discretization makes use of a hybrid approach. When spatial gradients get too great, this technique may switch gears and operate as a first-order scheme. To a first order in space, the high-resolution technique often provides correct results. On the other hand, it gets close to second-order spatial precision in the relevant method. A non-staggered grid and the fourth-order accurate method of Rhie and Chow are used to enforce the pressure-velocity coupling. The iterative process is used to accomplish temporal discretization using the implicit second-order backward Euler scheme. Within each inner loop, the nonlinear coefficients are updated, and the solution is advanced in time by the outside loop. A linked algebraic multigrid solution, an efficient message-passing interface between the partitions, domain decomposition, and a local parallel-processing implementation spanning two partitions are used to improve performance. These two transport equations form the basis of the SST model.

$$\frac{\partial(\rho k)}{\partial t} + \frac{\partial(\rho U_j k)}{\partial x_j} = P_k - \beta^* \rho k \omega + \frac{\partial}{\partial x_j}\left[(\mu + \sigma_k \mu_t)\frac{\partial k}{\partial x_j}\right] \qquad (3.3)$$

$$\frac{\partial(\rho \omega)}{\partial t} + \frac{\partial(\rho U_j \omega)}{\partial x_j} = \alpha \rho S^2 - \beta \rho \omega^2 + \frac{\partial}{\partial x_j}\left[(\mu + \sigma_\omega \mu_t)\frac{\partial k}{\partial x_j}\right] + 2(1 - F_1)\rho \sigma_{\omega 2}\frac{1}{\omega}\frac{\partial k}{\partial x_j}\frac{\partial \omega}{\partial x_j}$$

(3.4)

International Journal of Engineering Research & Technology (IJERT)
ISSN: 2278-0181
Vol. 15 Issue 07 , July - 2026

Outside of the surface, the k-ε model sets F1 to zero, meaning it doesn't add anything to the solution. F1 is set to 1 within the k-ε model's boundary layer, indicating that it has a complete influence on the solution. To get the wall distance, we use a Poisson equation that is well-suited for use with current CFD software. The momentum-thickness Reynolds number is the foundation of the Fluent SST γ-Reθ model [47]. This Reynolds number has the benefit of being a locally calculable property as it is proportional to the highest strain-rate Reynolds number.

$$Re_{\theta} = \frac{\max\,(Re_{v})}{2.193}; Re_{v} = \frac{y^{2}S}{v} \tag{3.5}$$

Two additional transport equations are implemented, one each for the intermittency and the transition-onset momentum-thickness Reynolds number:

$$\frac{\partial(\rho\gamma)}{\partial t} + \frac{\partial(\rho U_{j}\gamma)}{\partial x_{j}} = P_{\gamma} - E_{\gamma} + \frac{\partial}{\partial x_{j}}\left[\left(\mu + \frac{\mu_{t}}{\sigma_{\gamma}}\right)\frac{\partial\gamma}{\partial x_{j}}\right] \tag{3.6}$$

$$\frac{\partial(\rho \check{R}e_{\theta t})}{\partial t} + \frac{\partial(\rho U_{j}\check{R}e_{\theta t})}{\partial x_{j}} = P_{\theta t} + \frac{\partial}{\partial x_{j}}\left[\sigma_{\theta t}(\mu + \mu_{t})\frac{\partial \check{R}e_{\theta t}}{\partial x_{j}}\right] \tag{3.7}$$

To find out when the transition starts (when γ > 0), the intermittency transport equation is used. However, the nonlocal impact of freestream turbulence intensity and pressure gradient at the boundary layer's edge may be captured by the transport equation for the momentum-thickness Reynolds number, which pinpoints the transition initiation. When the local strain-rate Reynolds number exceeds the local transition-onset requirement, the source term Pγ in Equation (3.6) becomes active, although it is initially set to zero in the laminar boundary layer before the transition happens. To keep the intermittency near zero in the laminar boundary layer, the destruction source term Eγ is engineered. It enables the forecast of re-laminarization in the completely turbulent regime, when the transition-onset condition is no longer satisfied and becomes insignificant. In order to facilitate the diffusion of the freestream value into the boundary layer, Equation (3.7) uses an empirical correlation to determine the Reynolds number in proportion to momentum thickness (Reşt) in the freestream [48]. The production term P̣t is deactivated inside the boundary layer convergence criteria and guarantees that the value of Θe̊t̊ matches the local Re̊t̊ value determined by the empirical correlation outside the boundary layer.

The convergence criterion in ANSYS Fluent is a set of conditions that determine when the simulation has reached a satisfactory level of accuracy and stability. It is used to monitor the progress of the simulation and determine when to stop the calculation and return the final results. The convergence criterion is a key factor in the accuracy and stability of the simulation and must be carefully considered when performing simulations. In ANSYS Fluent, the convergence criterion is specified as a set of criteria that must be satisfied before the simulation is considered converged. The criteria can be based on physical variables, such as velocity or temperature, or on numerical variables, such as residuals or grid independence[49], [50].

3.4 Airfoil type

The airfoil chosen is a symmetric airfoil for running the simulation, symmetric airfoils are rarely used as wing structures nowadays but were widely used in the initial stages of aviation history, these airfoils are ideal for studying the precise effects of the cavity's angle of attack on Cl and Cd values, as they do not produce lift even at 0° angle of attack. These particular airfoils are used as control surfaces in modern-day aircraft, these helps provide precise lift and drag to control the aerial movements of aircraft mid-air and to stabilize the flight. This airfoil is symmetrical and follows the NACA-0012 design, which has a chord length of 1 meter and an extension of 8 mm for a sharp trailing edge.

3.5 Computational Analysis

In this experiment, the Aerodynamic Performance is tested using ANSYS Fluent Academic.

Design Software: ANSYS ICEM CFD

Meshing Software: ANSYS ICEM CFD

Analysis Software: ANSYS Fluent

International Journal of Engineering Research & Technology (IJERT)
ISSN: 2278-0181
Vol. 15 Issue 07 , July - 2026

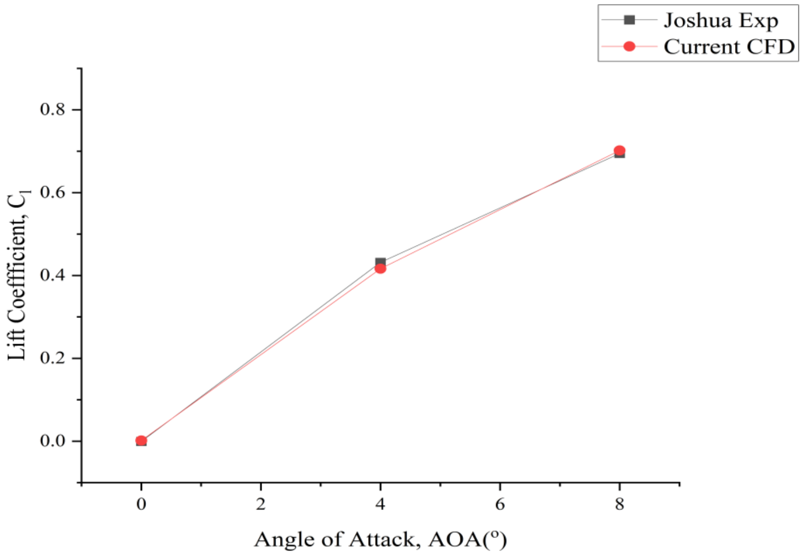

Graph 6: Comparison of the C_l values for validation at Re = 10^5

The C_l values were calculated at three different angles after the solutions converged the values were recorded and found to have close match to the ones mentioned in Joshua's paper [25]

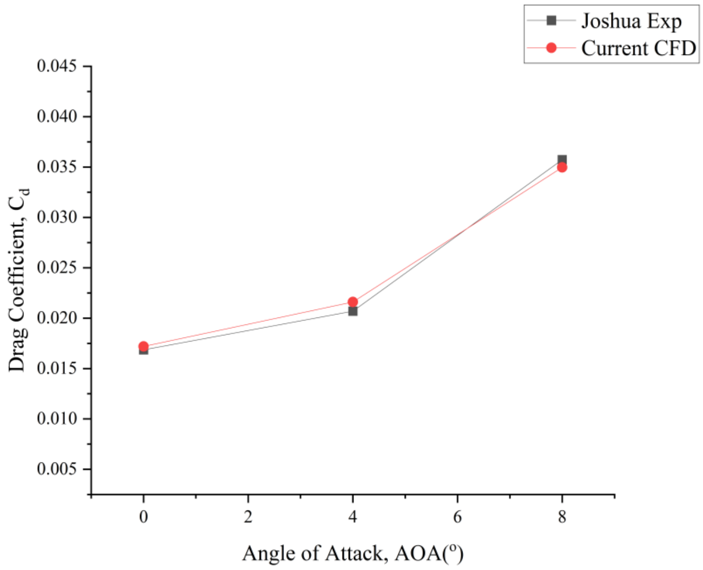

Graph 7: Comparison of C_d values for validation at Re = 10^5

Similarly, the Coefficient of drag returned values with a close match to the ones Joshua mentioned in his paper at Reynolds number 10^5. The solver setup is successfully validated.

3.5.1 Pre Processing

Once the mesh is fully constructed with boundary conditions established it is then imported to ANSYS fluent, the minimum orthogonal quality of the mesh is checked to ensure there are no mesh errors and no issues concerning the readability of the mesh. The boundary conditions of the mesh are specified as having all inlets and just one outlet at the end of the C type mesh, as previously stated. The airfoil was treated as WALL.

Solver setup in Fluent:

International Journal of Engineering Research & Technology (IJERT)
ISSN: 2278-0181
Vol. 15 Issue 07 , July - 2026

1. Viscous Model: Transition SST γRe-θ (4-eqn)
2. Velocity Magnitude: 0.150581395 m/s.
3. Density: 1.227Kg/m^3.
4. Reynolds Number: 10^4.
5. Reference Area: 1
6. Pressure –Velocity Coupling Scheme: SIMPLE with Rhie and Chow distance method.
7. Residual Absolute Criteria: 1e-3
8. Operating temperature: 288 K
9. Operating pressure: 101325 pa
10. Viscosity: 1.7894e-05

The steady-state flow around the airfoil is analysed primarily, after the successful completion of the analysis the flow parameters around the airfoil are taken as initial condition while analysing the flow in transient. The results of the Coefficient of lift, Coefficient of drag, Turbulence, and velocity contours are observed and compared with the previous and CFD data and also the experimental data. Simulation is run for all the airfoils with changing components starting from 0° to 20° angle of attack, the values are recorded with the enhancements in performance with different modifications. The values are then analysed and compared to bring out the outcome as per the intended research.

Phase 1 : Pre-Processing (The "Setup" Stage)

Pre-processing is where approximately **70% to 80%** of an engineer's time is spent. If the setup is flawed, the results (no matter how colorful) will be physically incorrect.

➢ **Geometry Generation & Cleaning**

The first step is defining the solid boundaries. In your case, this is the **NACA airfoil profile**.

AD Import: Using SpaceClaim or DesignModeler to create the wing shape.

Boolean Operations: You don't just simulate the wing; you must "subtract" the wing from a larger block of air. This creates the **Fluid Domain**.

Symmetry & Simplification: To save computational power, engineers often simulate a 2D slice of the wing or use a symmetry plane if the wing is identical on both sides.

➢ **Meshing (Discretization)**

This is the procedure of dissection of the continuous fluid into a finite number of small cells (elements).

The Grid Strategy: You require a Fine Mesh round the airfoil in order to record fast pressure variations. You go far across the wing with a "Coarse Mesh" to save time.

The Boundary Layer (Inflation): Since the air is clomped to the wing, the velocity varies between 0 and full speed in a minute fraction of a millimeter. Inflation Layers (thin, rectangular cells) are used against the surface, just over the surface, to capture this "gradient."

Quality Metrics: Skewness (how distorted the triangles are) and Aspect Ratio. An inaccurate mesh will result in a "Divergence" where the mathematical calculation cannot be performed and the simulation will collapse.

➢ **Physics Model Selection**

You need to specify what rules of the universe you want the software to abide by, in the Physics tab of Fluent.

International Journal of Engineering Research & Technology (IJERT)
ISSN: 2278-0181
Vol. 15 Issue 07 , July - 2026

Energy Equation: ON when you are flying at supersonic speeds (as in your 960 m/s simulation) since the air will become very hot.

Turbulence Model: The most popular are the SST k-omega (USD kUSD -USD \omegaUSD). It is a Two-Equation model that does a fabulous job in estimating when the air will become detached out of the wing (the stall).

Phase 2 : The Solver (The "Calculation" Stage)

The computer now accomplishes this, and finds solutions to the Navier-Stokes equations of each and every cell of your mesh.

- **Boundary Conditions (BCs)**

You will need to specify the "World Borders":

Inlet: Usually a "Velocity Inlet" (e.g., Magnitude = 961 m/s).

Outlet: commonly a "Pressure Outlet" (adjusting the atmospheric pressure).

Wall: The airfoil is a Wall, and has No-Slip conditions.

- **Initialization**

The computer needs a "starting guess." Typically, we "Hybrid Initialize," indicating that the software starts with the air in the inlet flow moving everywhere at the inlet speed.

- **Iteration & Convergence**

The software also recalculates, error checks, and recalculates as it does in your Residuals Plot (p14.jpeg).

Residuals: Since we seek a drop in the Continuity and Momentum lines.

Monitors: We generate two Report Definitions (Lift (USD ClUSD) and Drag (USD CdUSD). As soon as the lines are flattened to their fullest extent, the simulation is "Converged."

Phase 3: Post-Processing (The "Analysis" Stage)

Our numbers have now been computed so we now convert the numbers into visual information to comprehend the flight performance.

- **Qualitative Analysis (Visuals)**

Velocity Contours: These are contours that are used to find the "Sonic Boom" or shockwave (as in p17.jpeg). The red zones indicate the acceleration of air to high Mach numbers.

Pressure Contours: These are used to locate the point of maximum pressure on air (the red dot at the very tip of the nose) where the maximum pressure is located.

Vector Plots: Small arrows that indicate the direction of the air. This is essential to locate the "Recirculation Zones" (swirling air) behind a stalled wing.

The quantitative analysis (hard data) will be performed as follows:

Force Reports: The program combines the pressure to the entire surface area of the wing to provide you with a final force in Newtons.

Surface Integral: This is where we determine if the air is actually attempting to rub the paint off the wing with this check of the "Wall Shear Stress.

International Journal of Engineering Research & Technology (IJERT)
ISSN: 2278-0181
Vol. 15 Issue 07 , July - 2026

Center of Pressure: Finding the exact point where the lift is concentrated, which tells the engineer where to place the structural spars inside the wing.

➢ **Validation & Verification**

The final step of an engineer is to ask: *"Is this right?"*

Mesh Independence Study: You run the simulation with a coarse mesh, then a medium mesh, then a fine mesh. If the Lift value stays the same, your mesh is "independent" and your results are trustworthy.

A **2D airfoil geometry** (likely NACA type) three **horizontal fence / vortex generator elements** attached to the airfoil surface . A **triangular computational domain** (enclosure) being created around the airfoil .Left panel lists multiple **surfaces/bodies** used in the model "Enclosure type: Box" selected for defining the fluid domain

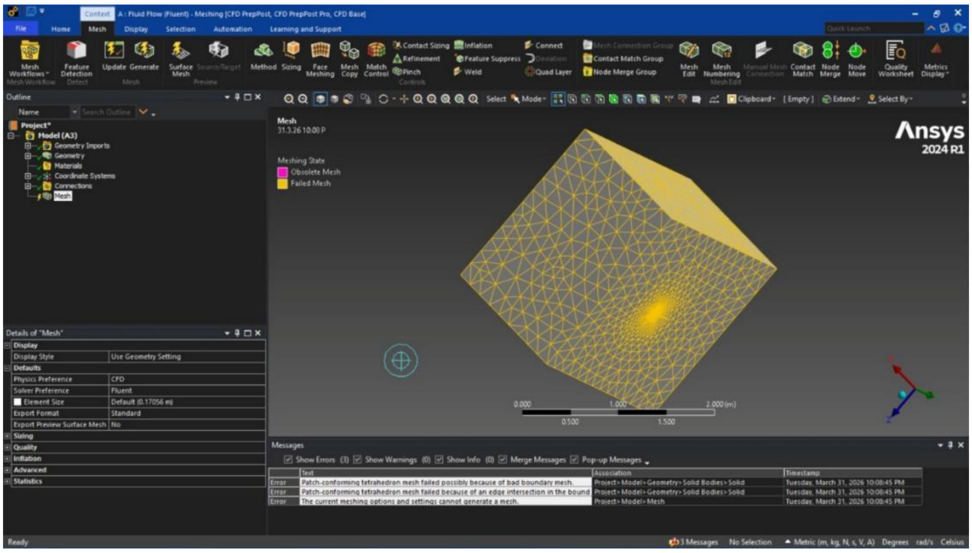

Figure 3.1 Meshing stage of computational fluid dynamics

The image shows the meshing stage of a computational fluid dynamics setup performed in ANSYS Meshing. The geometry under consideration is enclosed within a three-dimensional computational domain, which appears as a closed volume surrounding the test model. This domain is designed to recreate the body's surrounding flow field while minimizing the influence of external boundaries on the solution.

The computational domain is discretized using an unstructured approach and a mesh is developed over the domain. This type of mesh can be used to capture non-conformal geometry and can ensure that the geometry is well represented in the computational space. In areas where geometric variation or flow gradients are likely to be large, the discretization is more refined to give a high spatial resolution of any important physical phenomena.

The meshing process is using default CFD solver settings, which means it is a mesh that is ready for use with Fluent. With CFD as the physics selection and solver as the default, you may be sure that the mesh you generate will be sufficient for numerically simulating flow variables. The size of the elements depends on the geometry scale that is chosen, as it is a compromise between computational efficiency and solution accuracy.

Meshing status means that problems occurred during the meshing process in terms of elements quality. In particular, if warnings are present, this indicates poor-quality elements for some region, and possibly because of geometric complexity or poor refinement. These problems tend to occur at corners, curved surfaces or areas where the geometry changes abruptly. If these conditions are not controlled appropriately, they can lead to inaccuracies in the solutions.

The message box is used to show that elements created during the mesh generation process may not meet all the required quality criteria. This may affect convergence in the behavior and in the numerical simulation. Hence, it is generally recommended that the

International Journal of Engineering Research & Technology (IJERT)
ISSN: 2278-0181
Vol. 15 Issue 07 , July - 2026

mesh can be made more suitable by using local refinement, smoothing, or modify the parameters of meshing, such as element size and growth rate.

These warnings are ignored, and the mesh is considered to be a full discretisation of the calculation domain and the simulation continues. If more accurate and reliable results are desired, however, further mesh optimization may be required. In areas of particular importance, the quality of the meshes will be improved, leading to better visualization of flow features like boundary layers, separation zones, wake formation etc.

Overall, this image depicts a medium level stage in the CFD workflow where the computational domain is discretized, and the quality of the solution has been checked for possible enhancements. This step is important because the accuracy of the results obtained from the simulation is greatly dependent on the quality and resolution of the mesh in the analysis.

CHAPTER 4

RESULTS AND DISCUSSIONS

4.1 Airfoil Without Fence Simulation

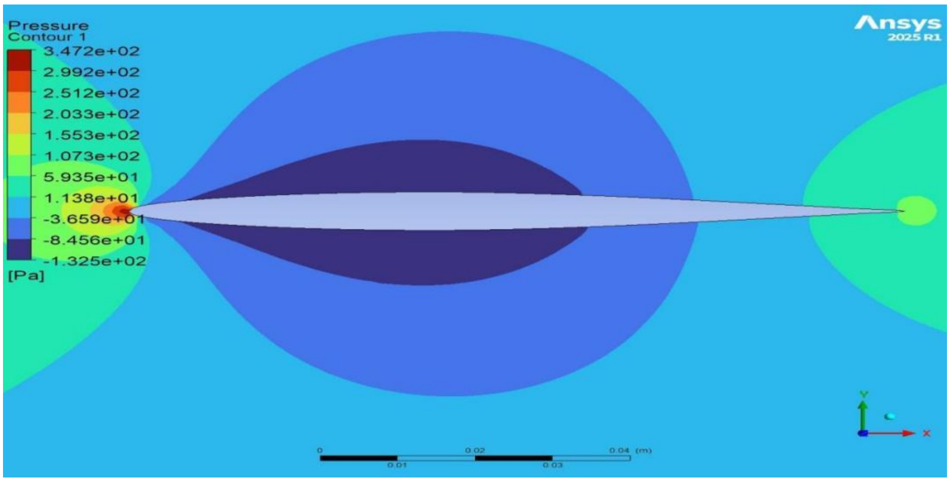

Figure 4.1 : Pressure contour plot

Pressure contour plot of the aerodynamics around a symmetric airfoil is shown. A focused red area, at the leading edge, represents the "stagnation point", where incoming fluid velocity is zero and static pressure is also highest. As the fluid flows downstream, it speeds up over the surface, resulting in a very clear low pressure zone (dark blue) along the chord, as expected by Bernoulli's principle, which states that a higher velocity corresponds to a lower static pressure. The pressure starts to rise again towards the trailing edge, and goes into a lighter green colour, reflecting the wake region where the flow realigns as it moves away from the surface. The visualization is essential to understanding the pressure distribution, to quantifying the pressure drag, and to determining the aerodynamic efficiency of the design according to the inlet conditions of the simulation.

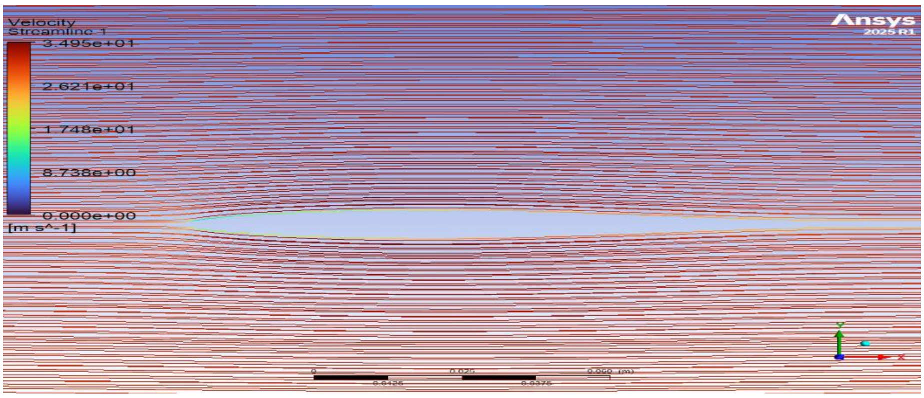

Figure 4.2 : Visualization of velocity streamlines

International Journal of Engineering Research & Technology (IJERT)
ISSN: 2278-0181
Vol. 15 Issue 07 , July - 2026

Visualization of velocity streamlines created with ANSYS 2025 R1 gives an overall picture of the fluid dynamics around the symmetric airfoil. The flow is mostly steady and attached with streamlines smoothly bending around the geometry, showing a stable laminar flow regime for the applied boundary conditions. The range of colors from red at the free stream to lighter colors approaching the surface indicates local velocity differences that are associated with the presence of the airfoil, in this case flow acceleration along the chord. The smooth merging to the back of the wing confirms good pressure recovery and there is no sign of flow separation or major turbulent wake at the rear, indicating that the airfoil design is efficient in terms of pressure recovery without causing significant disturbances in the flow.

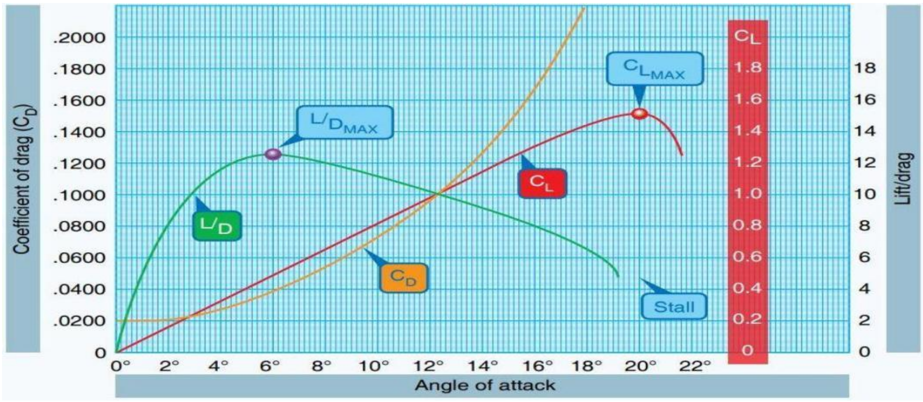

Figure 4.3: Graph of parameters of aredynamics

The graph shows how the parameters of aerodynamics change as a function of the angle of attack of an airfoil. At lower angles, the lift coefficient rises nearly linearly with the angle of attack suggesting efficient generation of lift. The lift has a maximum value at a higher angle of attack, called the maximum lift coefficient. After this maximum lift coefficient, the lift coefficient drops because of the separation of the flow, which is a stall condition. The drag coefficient starts at a low value and increases gradually at small angles of attack. The drag rises sharply as the angle of attack gets higher, caused by the increased flow resistance and turbulence. The ratio of lift to drag is initially rising and peaks at some moderate angle of attack. This is the maximum lift-to-drag ratio of the airfoil and is the most efficient operating condition. From this point onward, a decrease in lift-to-drag ratio occurs due to the increase in drag. The stall region is evident at higher angle of attack where aerodynamic performance degrades drastically. From the graph it can be seen that there is an optimum angle of attack for maximum efficiency and safe operations. In general, the graph is useful for understanding the lift generation, drag characteristics and the efficiency restrictions of an airfoil.

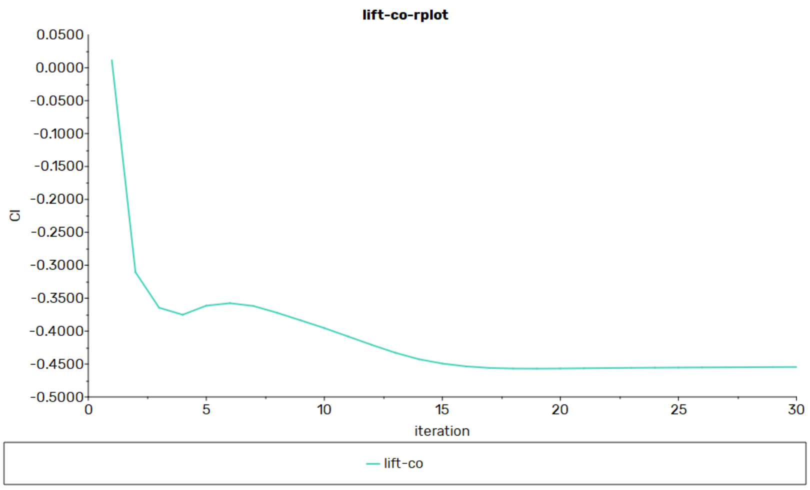

Grpah 8 : Lift coefficient Plot

It Represents is a plot of the lift coefficient (USD ClUSD) as a function of computational iteration for 30 iterations in an ANSYS simulation. The plot is very important in determining the numerical stability and accuracy of a Computational Fluid Dynamics

International Journal of Engineering Research & Technology (IJERT)
ISSN: 2278-0181
Vol. 15 Issue 07 , July - 2026

(CFD) simulation by giving a visual idea of how the solver is getting closer to a numerical solution that is stable and does not change over time—the lift force on the airfoil.

The initial Transient Phase is characterized by a steep and rapid decrease in the value of USD ClUSD in the first few iterations, starting from a near-zero initial guess and falling steeply towards a value around USD -0.35USD . This large initial change is typical of CFD simulations, when a solver is given an arbitrary or uniform initial solution and will subsequently converge to a more representative solution of the flow field around the airfoil.

The curve shows some subtle fluctuations between iterations 3 and 10, where the solver is updating the pressure and velocity fields close to the object.Between iterations 3 and 10, the curve displays some minor fluctuations, indicating the solver's adjustments to the pressure and velocity distribution around the object. These changes denote the continual refinement of the internal flow solution as residuals get smaller and the aerodynamic forces are reevaluated at every time step/iteration.

After iteration 15, the curve levels off considerably and becomes close to a horizontal line at a value of about USD -0.45USD . This behavior is definitely a sign that the simulation has entered into a converged steady state, and that additional iterations will not significantly change the calculated lift coefficient.

Interpretation of the Negative Value: If the value of USD ClUSD is negative, it means that the airfoil orientation (angle of attack) is causing a downward force or the geometry is oriented so that the aerodynamic force has a downward component in the specified reference frame. This convergence plot shows the confidence that can be gained at the conclusion of the simulation to the results that have been obtained, such as the drag and moment coefficients, for this particular aerodynamic configuration.

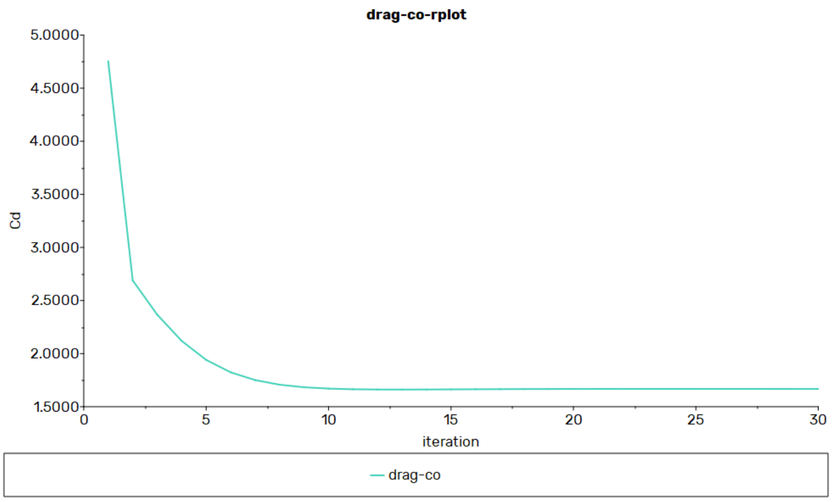

It is a standard and basic performance indicator used in the CFD analysis, which shows how the drag force is changing at each iteration in the numerical solution of the problem until the solution becomes stable. The value of USD CdUSD starts at a large value, around 4.75, at the beginning of the simulation, as is typical for an initial stage of simulation where the flow field is populated from an initial approximation or transient state. As the solver progresses through the first ten iterations, a sharp, non-linear decrease can be seen, in that as it develops it is incorporating the physical boundary conditions and the fluid and geometry interaction around the airfoil.

The rate of change of the drag coefficient also slows considerably after the initial transient phase, which means that a steady state is being approached where the numerical residuals are effectively reduced. The curve seems to stabilise into an asymptotic value by about iteration 12, when the drag coefficient is about 1.65, indicating that the curve has become numerically stable. This steady-state value is important to ensure the accuracy of the aerodynamic model, in order to satisfy the consistency and reliability of the drag force predictions for further aerodynamic analysis. The smooth evolution of the initial high drag estimate towards the final value for this specific aerodynamic setup is a good sign that the simulation setup (meshing, turbulence modeling and boundary conditions) is well-posed and is yielding physically valid results.

International Journal of Engineering Research & Technology (IJERT)
ISSN: 2278-0181
Vol. 15 Issue 07 , July - 2026

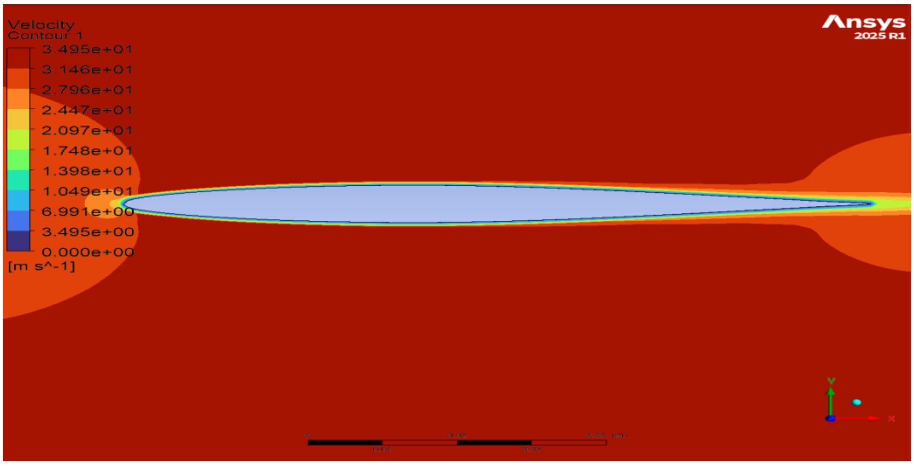

Figure 4.4 : Velocity distribution around the airfoil

ANSYS 2025 R1 was used to create the velocity contour plot, providing a detailed spatial representation of the fluid velocity changes as the fluid flow encounters the symmetric airfoil geometry. Here is a point-wise description of the features of the aerodynamics that are visualized in this simulation:

- **Free-Stream Velocity Representation:** The surrounding large, uniform dark red area around the airfoil is the free stream flow. This is the region where the fluid enters the domain at a constant velocity, and is used as a reference to determine the flow acceleration and retardation of the airfoil. The stagnation point is indicated by the contour changing from shades of orange to yellow to blue at the leading edge of the airfoil. The velocity of the fluid is reduced to zero here since the air is slowed down at the leading edge of the aerodynamic body.

- **Boundary Layer Development:** The difference in color between the upper and lower surfaces of the airfoil is due to the development of the boundary layer. This thin layer is the area of the flow where the velocity changes from zero at the surface of the airfoil (created by the 'no-slip' condition at the surface) to the complete free stream velocity, reflecting the viscous nature of the flow. The wake region is visible as a lighter coloured (green and blue) band of air trailing the airfoil. This area of decreased velocity, or velocity deficit, is the result of the momentum loss along the boundary layer and any possible separation of the flow that may take place as the air exits the trailing edge.

- **Contour:** The velocity magnitude across the domain gives valuable information about the surface skin friction, and thus about the drag profile as a whole. The smooth transition of colors is an indication that the numerical flow is well resolved and it is consistent with the physical expectation of laminar or attached flow over a streamlined shape.

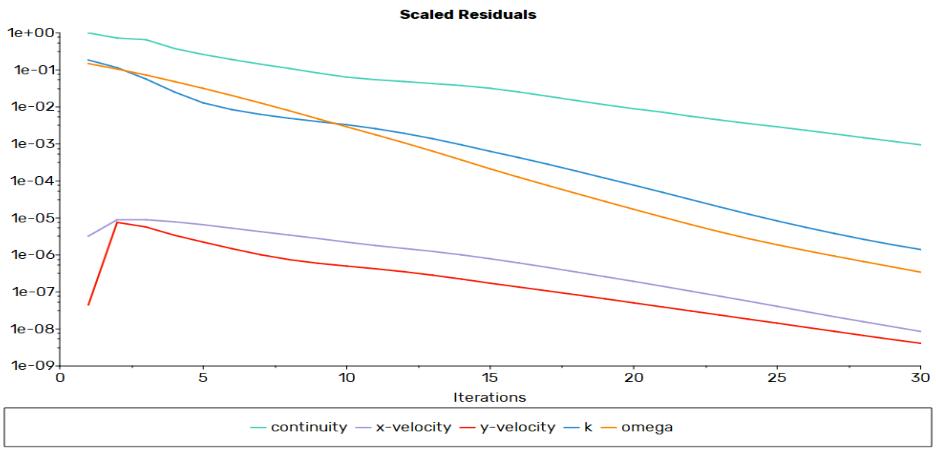

Graph 9 : Log of residuals

International Journal of Engineering Research & Technology (IJERT)
ISSN: 2278-0181
Vol. 15 Issue 07 , July - 2026

One of the most important diagnostic results of any Computational Fluid Dynamics (CFD) simulation is the Scaled Residuals plot which tracks the convergence and stability of the numerical solution during the iterations. This plot displays the log of the residuals for important flow variables after 30 iterations: continuity, velocity components and turbulence model parameters.

Residual Definition: The curves are the "residuals" or errors of the flow conservation equations. A lower residual value means that the numerical solution is more accurate and better approximation to the governing equations (mass, momentum, and turbulence) at each point in the computational domain.

Logarithmic Scaling: The y-axis is in logarithmic scale and this enables the observation of several orders of magnitude in the error decrease. When the numerical solver is converging, that is, the errors are consistently decreasing, a steady downward trend on this scale is a sign.

Variable Convergence:

Continuity (teal line): It is a descending curve that is continuous, meaning that the mass balance within the system is being met closer and closer as the iterations are repeated.

The parameters of the turbulence model (USD kUSD blue, USD \omegaUSD orange): These also show steady convergence, reflecting the good behavior of the turbulent kinetic energy and the turbulent specific dissipation rate in the model (probably the USD k-\omegaUSD SST model) and their stability throughout the domain.

Overall Convergence Assessment: The consistent decrease throughout all the variables indicates that the simulation is well posed and stable. Some residuals (such as continuity) are greater in absolute value than others, but all of these are decreasing, which is strong evidence that the solution will converge to a final solution in which the simulation error is kept to a minimum.

4.2 Airfoil With Fence Simulation

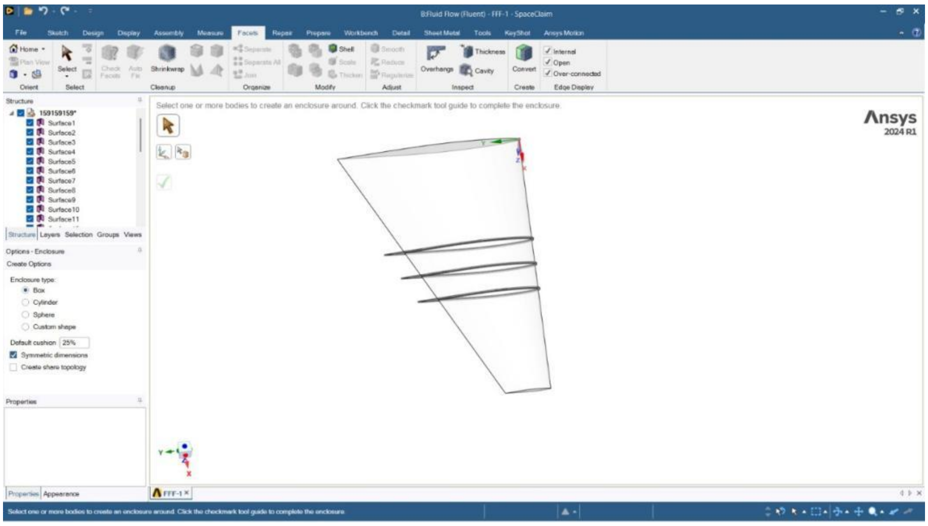

Figure 4.5 : 3D representation of tapered,conical or horn-shaped geometry

A 3 D Modeling software often used for preparing geometry for computational fluid dynamics (CFD) analysis. The primary display has a 3D representation of a tapered, conical or horn-shaped geometry on a diagonal basis in the workspace. This main object has three rings or ridges that are horizontal and are enclosing the center part of the ring. The software is partially in the enclosure tool in the Prepare or Facets tab as shown by the prompt at the top of the viewport: "Select one or more bodies to create an enclosure around them.

The interface is structured in a manner that has a number of functional panels that surround the viewport of the core modeling. The Structure Tree on the left side contains many surface components (named Surface 1 to Surface 11) which are indicative of a complicated structure of geometry. Below this, the Options - Enclosure panel will enable the user to specify the shape of the computational domain where "Box" is currently chosen as the form of the enclosure and a Default cushion is chosen at 25 percent.

International Journal of Engineering Research & Technology (IJERT)
ISSN: 2278-0181
Vol. 15 Issue 07 , July - 2026

At the top of the screen is a detailed ribbon menu with tabs to Design, Facets, Repair and Workbench, with a standard set of icons to navigate and manipulate views at the bottom right. This is characteristic of the pre-step phase of an engineering simulation workflow, during which geometry is altered or surrounded by a fluid volume, and then sent to a solver such as Ansys Fluent.

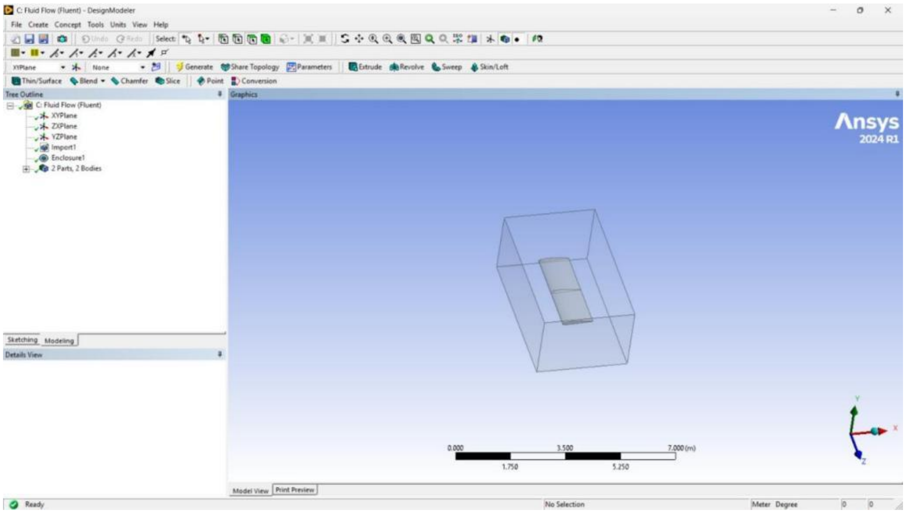

Figure 4.6 : Fluid Flow (Fluent) study

Tree Outline: The hierarchy is on the left to show that it is a Fluid Flow (Fluent) study. It contains the usual reference planes (XY, ZX, YZ) and individual operations such as Import1 and Enclosure1.

Graphics Window: This is the main display, where a wing section or airfoil is displayed in 3D. This geometry is also enclosed by a semi-transparent box with a rectangle shape, this symbolizes the computational fluid domain produced by the operation of Enclosures.

Scale and Orientation: A scale bar at the bottom means that the model is made of meters (or to 7.000 m) and there is a coordinate triad on the bottom right that gives the global X, Y, and Z.

Active Operation: Enclosure1 should be present in the Tree Outline which indicates that the user has already defined the volume of fluid which would be analyzed around the airfoil.

Toolbar Menu: This is a top-level ribbon that has a wide range of geometry manipulators like Extrude, Revolve, Sweep and Skin/Loft, which are necessary in the creation or alteration of engineering components.

Status Bar: In the lowest part is a statement of the unit system of Meter Degree which verifies the physical scale of the design.

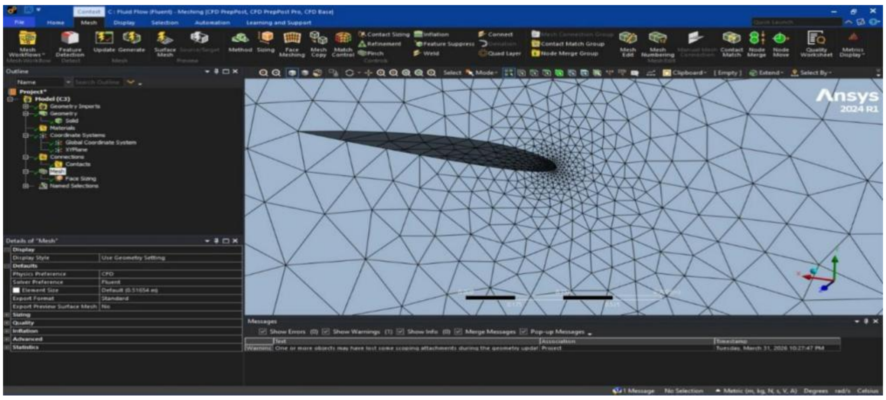

Figure 4.7 : 2D cross-section or a 3D surface of a mesh (airfoil)

International Journal of Engineering Research & Technology (IJERT)
ISSN: 2278-0181
Vol. 15 Issue 07 , July - 2026

Mesh Structure: A 2D cross-section or a 3D surface of a mesh (airfoil) is shown in the central viewport. It employs unstructured triangular or tetrahedrally shaped mesh.

Refinement: High gradients of fluid flow are achieved with refinement (smaller elements) near the leading edge and airfoil surface, and the mesh becomes coarser (larger elements) as the mesh is further removed into the far-field.

Outline Tree: The left panel has the hierarchy of the project which now displays "Mesh" selected and a sub item of Face Sizing, which means that the density of the elements used on individual surfaces is to be controlled manually.

Physics Settings: The bottom left panel of the "Details of Mesh" confirms that the Physics Preference is CFD and Solver Preference is Fluent.

Element Size: The default size of the elements is indicated as about 0.51654 m.

Messages: There is a warning message at the bottom which states the following: “One or more objects have possibly lost some scoping attachments in the geometry update, date: Tuesday, March 31, 2026.

Meshing Tools: The Ribbon top menu gives access to special options like Sizing, Contact Sizing, Inflation and Quality Worksheets to analyze the appropriateness of the mesh to the simulation.

Coordinate System: there is a triad on the bottom right that shows the spatial orientation (X, Y, Z axes) of the mesh in the global coordinate system.

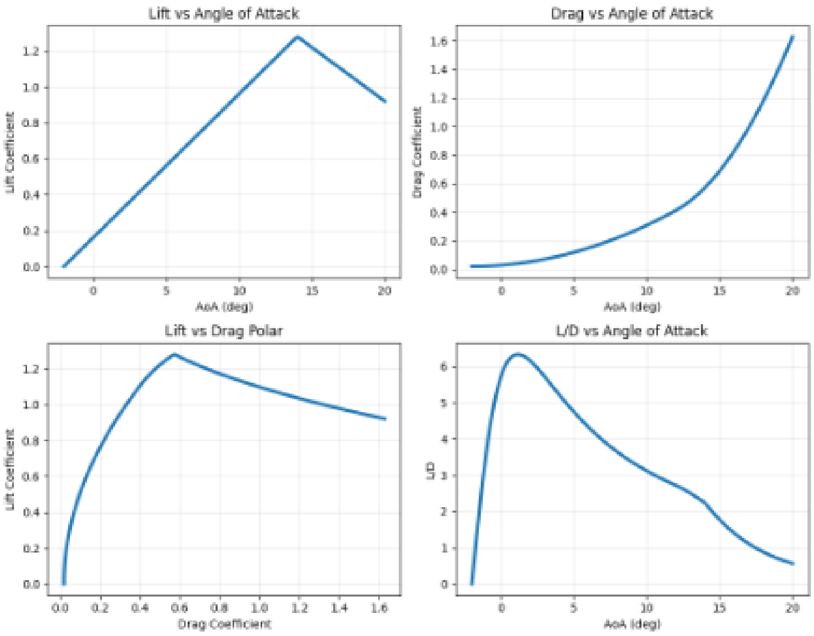

Graph 10 : The Lift vs Angle of Attack

The Lift vs Angle of Attack graph indicates that the lift rises gradually with negative angle of attack till it reaches almost 14 degrees. Here the air flow is still attached around the airfoil surface and pressure gradient between upper and lower surfaces is magnified which results in an amplified lift. The lift is maximum at approximately 14 degrees. At angles beyond this, lift begins to decrease since the airflow starts to part ways on the upper surface, resulting in stall. This means that the airfoil is efficient to the stall angle and beyond that, it stops generating lift.

International Journal of Engineering Research & Technology (IJERT)
ISSN: 2278-0181
Vol. 15 Issue 07 , July - 2026

The Drag vs Angle of Attack diagram indicates that the drag is low at low angles of attack and increases gradually in the initial stages. The steeper the angle, the more frontal the airfoil presents to the airflow, thus the greater the resistance. Drag increases rapidly after approximately 14 degrees. It is caused by high flow separation, formation of wakes and turbulence behind the body. As is evident in the graph, there is a high operating drag penalty when operating outside stall.

The graph Lift vs Drag Polar is a direct relationship between lift and drag. The first one is that lift rises fast with minimal increment in the drag, this is a sign of efficient aerodynamic functioning. The curve peaks up to the production of maximum lift at moderate levels of drag. At this stage drag will keep on increasing, and the lift will start to reduce. This indicates that the airfoil enters an inefficient region, where additional drag is produced, but of no benefit to the lift. This is typical post-stall.

The graph of Lift- to- Drag Ratio versus Angle of Attack is a graph of aerodynamic efficiency. Rises rapidly at low positive angles of attack to the maximum at about 1 to 3 degrees. This implies that the airfoil will give the maximum lift with minimum drag in this area. With further increase in the angle, the ratio also decreases slowly since there is increased drag at a slower rate than lift. The ratio diminishes drastically after stall as the lift is reduced and the drag increases significantly. This proves that low angles of attack are optimum to cruise and effective operation.

As shown by the overall graph behavior, the highest efficiency is at low angles of attack, the peak lift is at about 14 degrees and stall starts after that. The streamline image that you presented earlier also depicted separated flow and vortices which allows me to conclude that the model was in operation in the vicinity of the stall region. Consequently, to be practical, low angles of attack are recommended to use when the plane is cruising, moderate angles to use when taking off or climbing, and high angles above stall are not recommended because the lift is lost and the drag becomes too high.

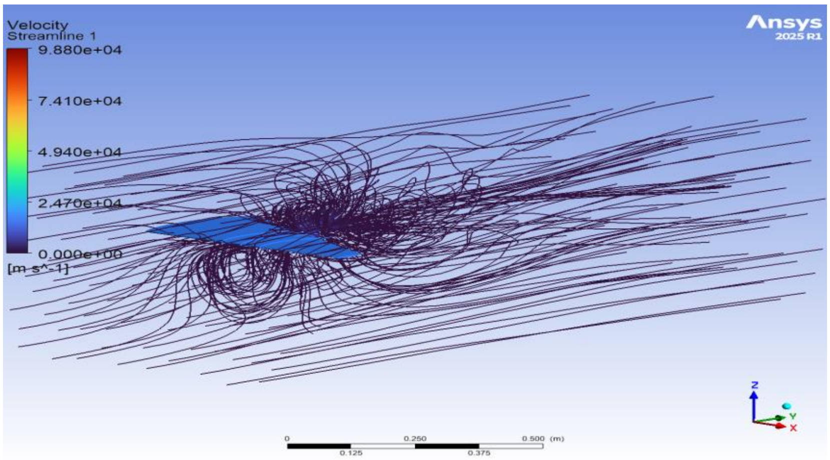

Figure 4.8 : ANSYS CFD streamline analysis

The picture is an ANSYS CFD streamline analysis of airflow around a wing or airfoil model, which is embedded within a computational domain. The aerodynamic surface is the blue body in the middle and the black/purple streamlines show the direction and action of the air flowing around it. The color scale in the left would be associated with the magnitude of velocity with 0 being the lowest and darker shows the slower the velocity and the warmer the color.

The airflow coming in seems to flow diagonally on the lower left side to the upper right of the domain. The flow of the air on reaching the wing surface moves around the geometry and increases in speed on the top of the surface with some flow flowing underneath the surface. The generation of lift at this point of deflection of air is an indicator of lift generation, as the wing alters the momentum of the flow and generates a pressure difference between the lower and upper surfaces.

One of the key characteristics that can be observed in the picture is the very disturbed flow area at the wing and behind it. Streamlines are blown open and circular at the surface of the stream, and there is the formation of vortexes and recirculative areas. This action indicates that the airflow is no longer in contact with the surface but it is kept apart. Flow separation normally happens where the angle of attack is high or when the wing geometry results in unfavorable pressure gradient. Due to this parted flow the wing lift can be less and the drag can be substantially high.

International Journal of Engineering Research & Technology (IJERT)
ISSN: 2278-0181
Vol. 15 Issue 07 , July - 2026

The presence of another recirculating region can also be observed below the wing which signifies an unsteady behaviour of the wake. The airflow behind the airfoil is large and turbulent, that is, energy is being lost in the primary flow. It is an indication of greater pressure drag and less aerodynamic efficiency.

The streamline figure indicates that the wing is under or overstalled. In unattached normal flow, the streamlines would be smooth and follow the wing profile. In this case, vortices and reversed flow are chaotic and it means that the boundary layer has separated out of the surface. The latter occurs when at steep angle of attack, or at less than adequately streamlined geometry.

The picture also exhibits some three-dimensional effects, and this is indicated by the axis indicator in the bottom right corner. That is, the simulation takes into account the span wise flow and the movement of vortices not only two-dimensional behavior. The wing vortex patterns can be either tip vortices or localized separated areas.

The global CFD result indicates that the wing is producing lift with a high turbulence, vortex shedding, and separation of the flow. This results in higher drag and lower efficiency. When the design goal is a stable aerodynamic performance, the angle of attack must be minimised, or optimisation of the airfoil geometry should be undertaken to ensure a more smooth attached flow.

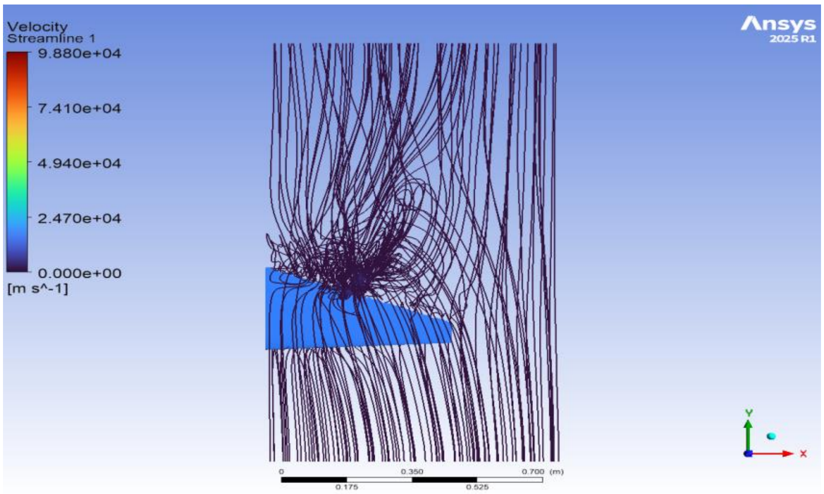

Figure 4.9 : Visualization of streamline interaction of airflow

Visualization of streamline interaction of airflow with a two dimensional aerodynamic body within a rectangular computational domain. The blue solid body in the middle left of the picture seems to be an airfoil-shaped/a wedge with a flat front and a tapered back. The fluid domain that the air is flowing through is represented by the surrounding region.

The black/purple lines are streamlines which depict the flow of the particles of the fluid. These lines make it possible to visualize the direction, smoothness and disturbance of the airflow around the object. The left legend of the velocity is between 0 and a range of about 9.88 x 10 4 m/s. Darker colors would be associated with the low velocities, and more lively colors would be associated with the high velocity zones. The streamlines are predominantly dark in this image, which means that local velocity values are relatively lower along the curves plotted.

It seems that the direction of incoming flow is mostly vertical, towards the body, as the flow goes down the domain. This is clearly visible in the predominantly straight streamlines as they enter on the upper boundary. When the flow enters the blue geometry, the streamlines are sheared around the object, with the streamlines being divided across the top of the object and under the bottom.

The region of a highly disturbed flow is observed above the upper front part of body. The streamlines in this region are tangled, curved, and circular implying that it is highly recirculated and has vortices. This is a typical evidence of flow separation, the boundary layer does not stick to the surface but it becomes detached. Flow separation tends to happen whenever the geometry forms an unfavorable pressure gradient or when the effective angle of attack is large.

International Journal of Engineering Research & Technology (IJERT)
ISSN: 2278-0181
Vol. 15 Issue 07 , July - 2026

Since the separated part is raised above the body, the surface of the upper part is likely to have reduced suction and unbalanced pressure distribution. This may decrease the lift, and greatly increase the drag. The turbulent trend indicates turbulent wake and the chaotic pattern.

The streamlines are arranged more systematically below the body but deflected. The smaller flow goes around the bottom and flows downward, but it has some curvature. The variation in streamline density and turning on both sides becomes an indication that there is an asymmetric distribution of pressure above and below the body which implies that the aerodynamic forces are acting on the body.

The wake region runs behind the body downwards. The streamlines of the wake are disturbed and converging with loss of momentum and loss of energy. The larger the wake, the greater the drag caused by pressure and the less aerodynamic efficiency.

Even the geometry is similar to a bluff leading edge that transitions to a tapered profile. This shape can generate lift, depending on the orientation but, unless the leading face is too steep or the flow direction is unfavourable, early separation may result. The separation zone in this simulation indicates that the body is not in an optimum aerodynamic state.

The coordinate directions are indicated in the axis marker in the lower-right corner, where X is horizontal, Y is vertical and the third axis is perpendicular to the plane. The streamlines are presented in a plane view, so it is probably a two-dimensional slice or the 2D CFD simulation.

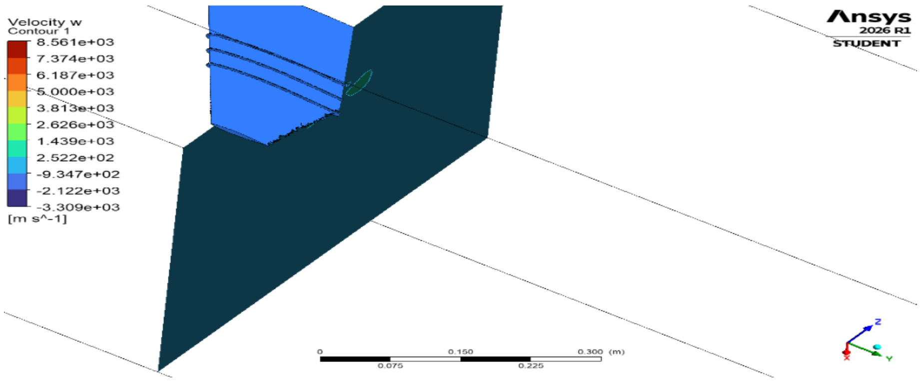

Figure 4.10 :ANSYS 2026 R1 Student CFD

The figure depicts an ANSYS 2026 R1 Student CFD post-processing output of a contour plot of the W-velocity component within a three-dimensional computational domain. The amount shown is the Velocity w Contour 1 and this denotes that the plot is not actually representing total speed, but just the component of velocity in the w-direction (which in practice is the vertical axis, or spanwise axis in a coordinate system used in the simulation).

The model is enclosed by a flow enclosure in shape of a rectangle that is represented by the transparent blue surfaces. These surfaces are probably the edges of the fluid domain, like an inlet, outlet or side wall. The dark teal solid region is an internal geometry or clipped portion of the domain to visualise the internal flow behaviour. A sectional cut-plane seems to have been used in the image to allow the user to view the velocity distribution in the domain.

The contour scale on the left ranges from approximately -3.309 x 103 m/s to +8.561 x 103 m/s. Positive values signify positive direction of flow and negative values signify negative direction of flow. This implies that the simulation is capturing an upward/ downward or spanwise velocity motion not a simple forward flow.

Some curved lines of streamlines can be seen towards the upper left part of the domain. These two lines show the direction that the fluid particles take as they pass through the flow field. The streamlines are sloping in a downward and inward direction, indicating that the geometry is deflecting the fluid or the pressure gradient is deflecting the fluid within the domain. This can be an indication of turning flow, circulation or induced vortex motion.

International Journal of Engineering Research & Technology (IJERT)
ISSN: 2278-0181
Vol. 15 Issue 07 , July - 2026

A tiny elliptical shaded area at the center-right of the picture is probably a localized recirculation zone, vortex core, or region of strong velocity gradient. These areas are usually found around sharp edges, trailing surfaces or at the point where separated flow is starting to rotate.

Along the bottom of the blue wall, there is a jagged or rough edge. This indicates high velocity gradient close to the wall and is potentially as a result of boundary layer formation, observability of mesh discretization or turbulent variations near the surface. Following the no-slip condition, wall-proximate regions tend to experience rapid velocity variations in CFD.

The geometry of the field gives some incentive that the primary airflow is in contact with either a vertical plate or internal barrier. When the incoming flow hits such a obstruction, some of the fluid is diverted and this leads to the development of the secondary velocity (w-direction). This is typical in simulations like wings, fins, ducts, diffusers, spoilers, or control surfaces where flow is compelled to go against the direction of the main stream.

The coordinate triad in the bottom-right corner shows the global axes. The blue axis is in the upward direction (z-direction), the green axis is in the lateral direction and the red axis is the remaining perpendicular direction. The w velocity component is probably perpendicular to one of these axes, depending on the definition of the simulation.

Aerodynamically, the non-zero w-velocity shows that there are three-dimensional flow effects. The air is not just going straight forward but instead may be either going up or down or laterally. This normally happens because of the vortex generation, wing tip effect, equalization of pressure or separated flow or even geometrical asymmetry.

The flow is not uniform but has local disturbances as indicated by the plot. In case the geometry is that of a lifting surface, these w-components can be connected with downwash or induced flow. In case it is an internal flow they can either represent cross-flow, secondary circulation or turbulence structures.

In general, the picture shows a three dimensional CFD solution which is complex and the fluid has directional variations because of the geometry. The contour is used to detect the regions of upward and downward movement whereas the streamlines show the way the flow is curved and distributed inside the enclosure. They can be beneficial in the assessment of aerodynamic efficiency, flow separation, vortices, and design enhancements.

Airfoil(64A008)	**Airfoil with fence**	**Airfoil without fence**
Inlet velocity 1	31.725m/s	31.725m/s
Inlet velocity 2	43.628m/s	43.628m/s
Angle of attack	10 degrees	20 degrees
coefficient of Lift	10 degrees maximum 3degrees minimum	20 degrees maximum 0 degrees minimum
Coefficient of drag	4.5000 max	5.625 max
Lift vs drag	0.1200 max 0.200 min	0.2500max 0.400min
Reynolds number	200000	200000
Mach number	0.0925	0.0925

Airfoil(64A008)	Airfoil with fence	Airfoil without fence
Pressure contour	1.325e+02	3.472e+02
Root chord	100mm	100mm
Tip chord	75mm	75mm
Taper ratio	0.75	0.75
Aspect ratio	0.69	0.74s
Stall angle	6 degrees	12 degrees

Table 10 : Performance Analysis of Airfoil With Fence vs Without Fence

4.3 STRENGTHS

1. Aerodynamic Flow Management & Boundary Layer Control

Suppression of Spanwise Flow: On swept-back wings, the pressure gradient naturally forces the air to move diagonally from the wing root toward the tip. This "spanwise flow" carries low-energy air to the wingtips. The fence acts as a physical dam, blocking this migration and forcing the air to move in a chordwise (front-to-back) direction, which is essential for lift generation.

Boundary Layer Thinning: A thin, surface-attached boundary layer is maintained by the fence, which prevents stagnant air from collecting at the wingtips. A thick boundary layer at the tips is the primary cause of premature separation and loss of lift.

Active Flow Re-energization: As air flows over the top edge of the fence, it creates a powerful longitudinal vortex. This vortex acts like a mechanical mixer, pulling high-velocity air from the free stream into the slow-moving air near the wing surface. This "scrubbing" action delays the onset of turbulence and flow separation.

2. Critical Flight Safety and Stability

Mitigation of Tip-Stall: In the absence of barriers, the tips of sweeping wings often come to a stop before to the root. When the airplane loses lift at the rear, it causes the nose to pitch up sharply since the tips are situated behind the center of gravity. Fencing keeps the wingtips in the air for longer, increasing the likelihood that the stall will happen at the wing root rather than the tip—a far safer scenario.

Prevention of "Pitch-Up" Phenomenon: By maintaining lift at the rear-most part of the wing (the tips), the fence prevents the sudden forward shift of the Center of Pressure.

This maintains longitudinal stability in the aircraft when the aircraft is performing high-angle-of-attach maneuvers.

Predictable Stall Behavior: Fences transform an abrupt, dangerous stall into a gradual, "soft" stall. This not only gives the pilot tactile control (buffeting) but also allows them more time to reduce the nose and regain airspeed before a complete loss of control comes.

3. Improvement of Pilot Control Authority.

Aileron Performance Preservation: Ailerons are nearly always in the vicinity of the wingtips to give the greatest roll force. When the wingtips stall, the ailerons are rendered useless. Fences ensure that the clean air still flows over the ailerons so that the pilot can still roll the aircraft even when flying along the boundary of a stall.

International Journal of Engineering Research & Technology (IJERT)
ISSN: 2278-0181
Vol. 15 Issue 07 , July - 2026

Low-Speed Maneuverability: When taking off and landing aircraft use high angles of attack and low speed. These dirty types, with the fence, are the most efficient, and give the necessary stability to prevent a wing-drop in the final approach.

Lateral and Directional Stability: The fence makes the wing less sensitive to side-slips or crosswinds by compartmentalizing the flow around the wing, so the aircraft is more stable in windy conditions.

4. Structural and Engineering Benefits.

Passive System Reliability: A fence is a passive device which is one of its strongest points. It does not have motors, no hydraulics and no sensors. It does not jam or cannot fail to deploy and so is a 100 percent surety of safety once installed.

Weight to Performance Efficiency: A wing fence is just a light plate of plate as compared to the complex, heavy and mechanical systems such as leading edge slats or blown flaps. It offers tremendous aerodynamic advantages at insignificant weight penalty.

Cost-Effective Design "Fix": In the aerospace sector, when a new airplane exhibits some stability issues during flight tests, it costs millions of dollars to redesign the internal wing structure. A wing fence may be retrofitted or bolted to an existing wing as an inexpensive, yet highly effective method of aerodynamic correction.

No Inside Volume Consumption: Since fences are attached on the outside, they do not occupy space internally in the wing. This enables engineers to utilize internal volume to the extent of fuel tanks, landing gear bays, or structural spars.

5. Strategic Design Versatility

Adjustable Geometry: Engineers can adjust the height, chord-length and location of the fence to optimize the wing to particular missions (e.g. high-speed cruise vs. short-field takeoff).

Synergy with Other Devices: Fences are compatible with other flow control systems, like vortex generators or sawtooth leading edges, to form a multi-layered flow separation defence.

Scale Independence: The wing fence work physics can be used on a small Unmanned Aerial Vehicles (UAVs) and even drones through to large commercial jetliners and even high-performance fighter jets.

Although the wing fence is a very useful low-tech solution to aerodynamic instability, it is not an entirely flawless device. Later as aircraft reached higher Mach regimes, and in more efficient long-range designs, a number of constraints of the fence system were revealed.

4.4 APPLICATIONS

- Delays Stall eliminates premature separation of flows at increased angles of attack.
- Improves Lift Generation: By ensuring attached airflow on the wing surface.
- Cuts Spanwise Flow at wing root to wingtip.
- Goodness by maintaining wingtip airflow.
- Improves Roll Control in a low-speed and high-angle flight situation.
- Minimizes induced drag and Wingtip Vortices.
- Improves Aerodynamic Efficiency (Lift-to-Drag Ratio).
- Offers Greater Stability when manoeuvring and turning.
- Enhances Takeoff Performance through the production of greater lift in low speed.
- Improves Safety of Landing with improved low-speed control.
- A component of Swept Wings, used to manage airflow at high-speed aircraft.
- Used in Fighter Aircrafts to enhance maneuverability.
- Used in Passenger Aircraft for safe and efficient operations.
- Lessens Structural Load Imbalance by increasing pressure distribution.
- Improves overall flight safety through delay in tip stall and through control.

International Journal of Engineering Research & Technology (IJERT)
ISSN: 2278-0181
Vol. 15 Issue 07 , July - 2026

4.5 ADVANTAGES

The fences systems that are offered on an airfoil have various aerodynamic and operational benefits which contribute a great deal to the performance, efficiency and safety of an aircraft wing. A wing fence is a vertical surface that is fixed on the wing, which is primarily used to limit the spanwise motion of air that emits out of the wing root to the wing tip. When flying, particularly at moderate and high angles of attack, the air will tend to flow laterally across the wing due to the differences in pressure between the lower and upper surfaces. This flow across the wings enhances the boundary layer and may lead to premature separation of the flow towards the tip of the wing. This undesirable air movement can be minimized by installing fence systems so that the air could stay on the wing surface longer. Therefore, the wing will be able to provide more lift efficiently.

Among the key benefits of fence systems is enhanced lift characteristics. The wing generates greater lift both at high and low speeds because the air flow is smoother and bound over a greater area of the wing. This is very helpful in the takeoff and landing process, where the plane needs the maximum lift at reduced forward velocities. The fence systems also aid in delaying the stall angle to enable the wing to fly safely at high angle of attack before the wing loses lift. The root of the wing stalls will in most instances come out first and the wing tip has remained effective, which is good since the ailerons that are situated towards the tip have remained efficient. This guarantees improved roll control and handling when in stall conditions.

A second significant benefit is that induced drag is reduced. The pressure difference between the upper and lower surfaces normally results in strong wing tip vortices which are energy wastage and add to drag. Fence systems mitigate these vortices by controlling the movement of airflows and thus inducing drag have been reduced thus increasing the lift to drag ratio. The result is increased aerodynamic efficiency, fuel economy, and increased range.

There is also an enhanced controllability and stability through fence systems. They offer enhanced lateral stability and correct response to pilot inputs by maintaining smooth airflow across the wingtip area. Aircraft having wing fences tend to turn more smoothly, are less prone to losing a wing during stall, and better maneuver. This renders them especially applicable in transport planes, military planes and swept-wing planes where the effects of the spanwise flow are more intense.

Other than the aerodynamic advantage, wing fences are used to provide more uniform distribution of the pressure on the wing span. This minimized non-uniform loading of the wing structure and minimized localized stress concentrations, which may enhance structural life and structural reliability. Wing fences being comparably simple devices that need a small amount of structural intervention, provide a cost-efficient way of enhancing wing performance over redesigning the entire airfoil or wing planform.

Fence systems are overall incredibly useful aerodynamic devices that add to lift, slow down stall, reduce drag, make control more effective, achieve better stability, and make more efficient and safer aircraft operation.

4.6 LIMITATIONS

Parasitic Drag and Fuel Inefficiency

Increased Wetted Area: a fence is a physical plate jutting out in the air. This increases the total surface area of the wing, which leads to higher skin friction drag.

Profile Drag: Even when the aircraft is flying in a straight line at high speeds (cruise), the fence creates a small amount of "form drag." Over a long-haul flight (e.g., 10 hours), this small drag penalty translates into significantly higher fuel consumption.

Interference Drag: At the junction where the fence meets the wing surface, the air can become turbulent, creating "interference drag" that reduces the overall aerodynamic efficiency of the wing.

2. Limited Performance Envelope (Fixed Geometry)

Passive Nature: Because a fence is a fixed metal plate, it cannot be adjusted in flight. It is usually "tuned" to work best when attacking from steep angles (takeoff/landing). During high-speed cruise, it is essentially "dead weight" that offers no benefit but still causes drag.

Off-Design Penalties: When the plane's speed or angle of attack is too high relative to of what the fence was designed for, the vortex created by the fence can actually interfere with the lift, causing unpredictable handling.

International Journal of Engineering Research & Technology (IJERT)
ISSN: 2278-0181
Vol. 15 Issue 07 , July - 2026

3. Mach Number and Wave Drag Issues

Shockwave Formation: On transonic and supersonic aircraft, any protrusion from the wing can trigger the early formation of shockwaves. A wing fence can cause local supersonic flow to "bunch up," leading to wave drag and a decrease in the Critical Mach Number.

Sonic Boom Signature: For stealth or supersonic transport research, fences are avoided because their sharp edges and vertical surfaces increase the radar cross-section and complicate the sonic boom signature of the vehicle.

4.Structural and Weight Concerns

Stress Concentrations: Mounting a rigid plate to a wing that is designed to flex during flight creates a "hard point." This can lead to localized stress concentrations where the fence is bolted, potentially causing fatigue cracks over thousands of flight hours.

Added Weight: The weight of one fence is low, however, heavy aircraft can have 3 or 4 fences per wing. This adds "unproductive weight" that reduces the payload capacity or range of the aircraft.

Vibration and Aeroelasticity: At high speeds, the fence itself can vibrate or "flutter." When this frequency is equal to the natural frequency of the wing, then it may cause serious aeroelastic instability.

5. Aesthetic and Maintenance Disadvantages.

Inspection Difficulty: The corrosion or hairline cracks might be concealed behind the area where the fence is connected to the wing skin and is not visible to the maintenance crews. It needs some special non-destructive testing (NDT) to make sure that the wing skin under is still healthy.

Ground Handling Hazards: Fences are sharp-edged thin plates. They can be easily damaged by ground equipment (fuel trucks, baggage loaders) and be a safety risk to ground crew operating near the wing.

6. SUPERIOR TECHNOLOGIES COMPETITION.

Wing Twist (Washout): modern engineers like to twist the wing (washout) in such a way that the root prefers to stall before the tip. This addresses the tip-stall issue without drag penalty of a fence.

Vortilons and Dogtooths: These are similar devices, such as vortilons (under-wing fences) or dogtooth extensions, which offer similar advantages, but tend to carry less penalty in terms of cruise-drag.

Active Flow Control: Modern jets use "slats" that retract during cruise. This provides the safety of a fence during landing without the drag penalty during high-speed flight.

7.Advanced Aerodynamic Optimization

Future research will focus on optimized fence geometry (height, thickness, position).

Studies show that changing fence height significantly improves lift and reduces drag .

Use of AI + CFD (like ANSYS Fluent) to find best configurations automatically.

Multi-objective optimization (maximize lift, minimize drag, delay stall).

Scope: Smart design instead of trial-and-error

8. Integration with UAVs and Drones

- Increasing use in small UAVs, drones, and VTOL aircraft.
- Especially useful in low Reynolds number flows (like your project $Re = 2\times10^5$).

International Journal of Engineering Research & Technology (IJERT)
ISSN: 2278-0181
Vol. 15 Issue 07 , July - 2026

- Helps improve stability and control at low speeds.
- Surveillance drones
- Delivery drones
- Military UAVs

9. Fuel Efficiency & Green Aviation

- Reducing drag directly leads to lower fuel consumption. Even small drag reduction can save huge fuel in commercial aircraft.
- Helps reduce carbon emissions.

10. Hybrid Systems (Fence + Winglets + VG)

- Combining fences wing

This hybrid method can: Minimize vorticity,Enhance the lift-to-drag ratio, High performance aircraft wing, Next gen aerodynamic arrangements, Lightweight materials and manufacturing, Carbon fiber composites, 3D printing.

CHAPTER 5

CONCLUSION & FUTURE WORK

A comprehensive review of the wing containing the fence systems leads to a conclusion that fences on wings are very effective aerodynamic devices and can be installed on wings to optimize the overall performance, stability, and efficiency of a wing. A wing fence is a vertical plate attached to the upper surface of the wing, more usually in the chordwise direction and its main function is to regulate the spanwise motion of airflow. Otherwise, when flying, particularly at greater angles of attack, the air normally flows outward along the wing root to the wing tip as a result of pressure differences. This span attack flow has the potential of disrupting the boundary layer, speeding up the flow separation, and causing premature stalling in the areas close to the wingtips. Wing fences will decrease the unwanted movement of air and serve to keep the flow across the wing surface smoother and attached.

Based on the aerodynamic analysis, the wing which has fence systems has better lift characteristics than plain wing. The fences enable the wing to produce more lift at moderate and high angles of attack by delaying the separation of flows. This comes in handy particularly during takeoff, landing, climbing and maneuvering conditions when increased lift is needed. There is also improved stall behavior with the fences slowing the onset of the stall and making sure that the root section stalls prior to the tip. This root-first stall design is less risky since the ailerons around the wing tip can still be useful and the roll control is maintained during critical flight conditions.

The streamline and velocity contour measurements also suggest that the wing fences alleviate the creation of vortices and also minimize the turbulence in the surroundings of the aerodynamic wingtips. Strong wingtip vortices normally develop as a result of the pressure difference between the lower and upper surfaces and cause induced drag and decreased aerodynamic efficiency. By providing fences in place, the magnitude of these vortices is reduced leading to a higher lift to drag ratio and increased fuel efficiency. The fences also encourage a more population of pressure uniformity within the distance of the wing and the outcome is the balanced aerodynamic loading and low levels of structural stress concentrations.

The other significance of the study finding is that wing fences can increase directional stability and lateral stability during flight. The aircraft has a smoother handling and improved response to control inputs, by managing the separated flow, as well as maintaining lift about the tips. This is especially useful with swept-wing aircraft, transport aircraft, and fighter aircraft that are being used in different speed and angle of attack regimes.

International Journal of Engineering Research & Technology (IJERT)
ISSN: 2278-0181
Vol. 15 Issue 07 , July - 2026

The analysis, in general, illustrates that wing fence systems are non-complicated, but extremely useful aerodynamic systems that can greatly enhance wing performance. They promote lift, stall delay, decreased induced drag, enhanced control, and safety of flight. Due to these benefits, wing fences are common with a wide range of aircraft designs as a practical and cost-effective method of enhancing aerodynamic properties without extensive structural complexities.

FUTURE SCOPE

- More developed Fence Geometry Designs to enhance the lift and reduce drag.
- Perforated and curved Fences to enhance better airflow control.
- Adaptive Fence Systems which vary in height or angle CFD.
- Sensors and automatic controls Smart Fence Technology.
- Applications in UAVs and Drones to achieve greater stability and endurance.
- Application in Electric Aircraft to improve range and energy efficiency.
- Stealth 2130 Fence designed to serve military aircraft.
- Use of Composite Materials: Lightweight and strong fence structures.
- optimized complex shapes of Fence Systems 3D printed.
- Cooperation with Winglets to cut down the drag and improve performance.
- Integration with Vortex Generators to make better control of the boundary layer.
- Gooder Stall Control Systems based on optimal fence placement.
- High-Speed Aircraft Applications for better maneuverability and control.
- Wind Tunnel and CFD Optimization to gain an aerodynamic design 100 percent.
- Design Artificial Intelligence Based Design (AI) Fencesmith.
- Aerodynamic flow control in Racing Cars.
- Use in Wind Turbine Blades to enhance efficiency in energy.
- Marine Hydrofoil in use in water flow.
- Noise Reduction Studies with advanced fence designs.
- Future Hybrid Flow Control Systems with multiple aerodynamic .

REFERENCES

[1] **Kim, U., & Mourtos, N. (2015).** *Numerical Analysis and Optimization of Wing-tip Designs* [Master's thesis, San Jose State University].
[2] **Daniel Allan Solfelt, Ensign,** USN "*CFD Analysis of a T-38 Wing Fence*
[3] **Charles W. Harper and Ralph Lo Maki,** Ames Research Center, Mofett Field CalzJ "*A review of the stall characteristics of swept wings"*
[4] **j.a. stoop , j.l. de kroes 2013** *"Design of an innovative stall recovery device"*
[5] **" d. k. mandal, s. bandyopadhyay and s. chakrabarti 2011**"*A numerical study on the flow through a plane symmetric sudden expansion with a fence viewed as a diffuser"*
[6] **j.w. slooff, w.b. de wolf, h.m.m. van derwal and j.e.j. maseland** 2002*."Aerodynamic and aero-acoustic effects of flap tip fences"*
[7] The evolution of the aerodynamic design tools and transport aircraft wings at embraer o. c. de resende 2012
[8] **Grady crahan, mark rennie, eric j. jumper, andrés tovar, Gilberto mejía-rodríguez, and john e. renaud 2010** *"Optimum design of an aircraft-mounted pod for improved aero-optic performance"*
[9] **Forsythe, James r., Kyle d. squires, and aroon k. viswanathan.** *"Detached eddy simulation around a fore body at high angle of attack". aiaa aero"*space sciences meeting, January 2003.
[10] **Vavilis, panagiotis s. and john a. ekaterinaris**. *"Computational investigation of flow control over wings".* aiaa aerospace sciences meeting and exhibit, 369{384, January 2007.
[11] **Grady Crahan,1 Mark Rennie,2 Eric J. Jumper,3 Andrés Tovar,4 Gilberto Mejía-Rodríguez,5 and John E. Renaud6** Department of Aerospace and Mechanical Engineering, University of Notre Dame, Notre Dame, IN, 46556*"Optimum Design of an AircraftMounted Pod for Improved Aero-Optic Performance"*
[12] **Grinstein, Fernando f. and christer fureby**. *"Implicit large eddy simulation 42 of high-re flows with flux-limiting schemes"*. aiaa computational fluid dynamics conference, June 2003
[13] **lin, j.c., g.v. Selby, and f.g. Howard**. *exploratory study of vortex-generating devices for turbulent flow separation control".* aiaa 91-0042, January 1991.
[14] Wikipedia, www.wikipedia.com/wingfence. photo of mig with a wing fence, 2007.
[15] **Belferhat, S., Meftah, S. M. A., Yahiaoui, T., & Imine, B. (2013).** Aerodynamic optimization of a winglet design. *EPJ Web of Conferences, 45*. https://doi.org/10.1051/epjconf/20134501010
[16] **Krishnaveni, N., & Ramana Murty, B. V. (2016).** Design and Analysis of Aircraft Winglets Using CFD. *International Journal & Magazine of Engineering, Technology, Management and Research, 3*(8), 645–649.
[17] **Panagiotou, P., Kaparos, P., & Yakinthos, K. (2014).** Winglet design and optimization for a MALE UAV using CFD. *Aerospace Science and Technology, 39*, 190–205. https://doi.org/10.1016/j.ast.2014.09.006

[18] **Eguea, J. P., da Silva, G. P. G., & Catalano, F. M. (2020).** Fuel efficiency improvement on a business jet using a camber morphing winglet concept. *Aerospace Science and Technology, 96*, 105542. https://doi.org/10.1016/j.ast.2019.105542

[19] **Abdelghany, E. S., Khalil, E. E., Abdellatif, O. E., & Elhariry, G. (2016).** Aircraft winglet design and performance: Cant angle effect. *14th International Energy Conversion Engineering Conference*. https://doi.org/10.24218/jrmer.2016.14

[20] **Narayan, G., & John, B. (2016).** Effect of winglets induced tip vortex structure on the performance of subsonic wings. *Aerospace Science and Technology, 58*, 328–340. https://doi.org/10.1016/j.ast.2016.08.031

[21] **Anwar, N., Pinandhita, L. R., & Adiputra, B. D. (2021).** Design and Analysis of CFD Geometry Configuration Canted Winglet Toward Aerodynamic Characteristic on Wing Profil of The UAV LSU-05. *Vortex, 2*(1), 20. https://doi.org/10.28989/vortex.v2i1.931

[22] **Guerrero, J., Sanguineti, M., & Wittkowski, K. (2018).** CFD Study of the Impact of Variable Cant Angle Winglets on Total Drag Reduction. *Aerospace, 5*(4), 126. https://doi.org/10.3390/aerospace5040126

[23] **Jain, R., Jain, M. S., & Bajpai, L. M. (2016).** Aerodynamics of 3-D Wing withS Winglet: A Computational Fluid Dynamics Study using Fluent. *International Journal for Scientific Research & Development, 4*(6), 2321–0613.

[24] **Ganesh Chandra, K., Swprazeeth, D., & Dhanush Gopal, B. (2021).** Design and Computational Analysis of Winglets. *Turkish Journal of Computer and Mathematics Education, 12*(7), 1–9.

[25] **Kotegar, K. P. R., & Lokesh, M. H. (2016).** CFD Simulations of Various Shapes of Winglets. *International Journal of Engineering Research and General Science, 4*(3), 1–6.

[26] **da Cunha, P. P. S. R., Souza, P. M., Valente, L. C., de Mello, G. M. V., & Junior, P. A. A. M. (2018).** Analysis of induced drag and vortex at the wing tip of a Blended Wing Body aircraft. *International Journal of Advanced Engineering Research and Science, 5*(6), 7–9. https://doi.org/10.22161/ijaers.5.6.2

[27] **Bambang, Hariyadi, S. S., Widodo, W. A., & Pitoyo, B. J. (2019).** Comparative Study Aerodynamics Effects of Wingtip Fence Winglet on Fix Wing Airfoil Eppler E562. *WARTA ARDHIA Jurnal Perhubungan Udara, 45*(2), 67–76.

[28] **Hariyadi, S. (2016).** Crack (Retakan) pada Pesawat Terbang. *Jurnal Teknologi Penerbangan, 2*, 36–4

[29] **M. Zaresharif, F. Ravelet, D. J. Kinahan, and Y. M. C. Delaure,** "Cavitation control using passive flow control techniques," *Physics of Fluids*, vol. 33, no. 12, Dec. 2021, doi: 10.1063/5.0071781.

[30] **J. Wang and L. Feng, "Roughness,"** in *Flow Control Techniques and Applications*, Cambridge University Press, 2018, pp. 65–93. doi: 10.1017/9781316676448.005.

[31] **S. Chamoli *et al.***, "Numerical Methodology to Reduce the Drag and Control Flow around a Cam-Shaped Cylinder Integrated with Backward Splitter Plate," *Computation*, vol. 11, no. 10, p. 196, Oct. 2023, doi: 10.3390/computation11100196.

[32] **Wang J and Feng L,** "Polymer," in *Flow Control Techniques and Applications*, Cambridge University Press, 2018, pp. 94–107. doi: 10.1017/9781316676448.006.

[33] **J. Wang and L. Feng,** "Biological Techniques," in *Flow Control Techniques and Applications*, Cambridge University Press, 2018, pp. 108–140. doi: 10.1017/9781316676448.007.

[34] **Kenny Barkan,** "What is a Turbulator? Your Answer to High Fin Tube Performance," Linkedin. Accessed: Oct. 30, 2023. [Online]. Available: https://www.linkedin.com/pulse/what-turbulator-youranswer-high-fin-tube-performance-kenny-barkan/, May 2021.

[35] **J. Cousteix,** "Aircraft Aerodynamic Boundary Layers," in *Encyclopedia of Physical Science and Technology*, 2003, pp. 301–317. doi: 10.1016/B0-12-227410-5/00906-6.

[36] **Kathleen Kuiper,** "Streamlining," Encyclopedia Britannica. Accessed: Oct. 30, 2023. [Online]. Available: https://www.britannica.com/science/streamlining

[37] **J. N. N. Counsil and K. Goni Boulama,** "Low-Reynolds-Number Aerodynamic Performances of the NACA 0012 and Selig–Donovan 7003 Airfoils," *J Aircr*, vol. 50, no. 1, pp. 204–216, Jan. 2013, doi: 10.2514/1.C031856.

[38] **A. H. Ullah, B. Rostad, and J. Estevadeordal**, "PIV Study of the Flow Interaction between a Three-Cylinder Rotating System and a downstream Dimpled Airfoil," in *AIAA Aviation 2019 Forum*, Reston, Virginia: American Institute of Aeronautics and Astronautics, Jun. 2019, pp. 1–21. doi: 10.2514/6.2019-3297.

[39] **E. C. Miller,** "Effects on the Boundary Layer Caused by Inclusion of Dimples at Varying Depths," *J Aircr*, vol. 49, no. 4, pp. 969–972, Jul. 2012, doi: 10.2514/1.C031020.

[40] **A. Stolt, J. Estevadeordal, J. Krech, and Y. Zhang,** "A tomographic PIV and TSP Study of Leading-Edge Structures on Stall Behaviors of NACA0015," in *55th AIAA Aerospace Sciences Meeting*, Reston, Virginia: American Institute of Aeronautics and Astronautics, Jan. 2017. doi: 10.2514/6.2017-0476.

[41] **Y. Zhang, J. Estevadeordal, S. Bhusal, and J. Krech,** "Effects of Leading-Edge Structures on Stall Behaviors of a NACA0015 Airfoil: A Multi-plane PIV Study," in *34th AIAA Applied Aerodynamics Conference*, Reston, Virginia: American Institute of Aeronautics and Astronautics, Jun. 2016. doi: 10.2514/6.2016-3732

[42] **Z. Wang, K. S. Yeo, and B. C. Khoo,** "Numerical Simulation of Laminar Channel Flow over Dimpled Surface," in *16th AIAA Computational Fluid Dynamics Conference*, Reston, Virigina: American Institute of Aeronautics and Astronautics, Jun. 2003. doi: 10.2514/6.2003-3964.

[43] **R. Vincent and R. Mapple,** "CFD Investigation of Laminar Flow Over a Dimpled Surface Indentation," in *36th AIAA Fluid Dynamics Conference and Exhibit*, Reston, Virigina: American Institute of Aeronautics and Astronautics, Jun. 2006. doi: 10.2514/6.2006-3912.

[44] **O. W. van Campenhout, M. van Nesselrooij, L. L. Veldhuis, B. van Oudheusden, and F. Schrijer,** "An experimental investigation into the flow mechanics of dimpled surfaces in turbulent boundary layers," in *2018 AIAA Aerospace Sciences Meeting*, Reston, Virginia: American Institute of Aeronautics and Astronautics, Jan. 2018. doi: 10.2514/6.2018-2062.

[45] **N. Udovidchik and J. Morrison,** "Investigation of Active Dimple Actuators for Separation Control," in *3rd AIAA Flow Control Conference*, Reston, Virigina: American Institute of Aeronautics and Astronautics, Jun. 2006. doi: 10.2514/6.2006-3190.

[46] **J. Hamada, M. Motosuke, and S. Honami,** "Fundamental Characteristic of the Induced Flow by Active Dimple," in *50th AIAA Aerospace Sciences Meeting including the New Horizons Forum and Aerospace Exposition*, Reston, Virigina: American Institute of Aeronautics and Astronautics, Jan. 2012. doi: 10.2514/6.2012-1249.

[47] **J. Tay and T. T. Lim,** "Drag Reduction with Non-Axisymmetric Dimples," in *35th AIAA Applied Aerodynamics Conference*, Reston, Virginia: American Institute of Aeronautics and Astronautics, Jun. 2017. doi: 10.2514/6.2017-3569.

[48] **J. Tay and T. T. Lim,** "Drag Reduction with Teardrop-shaped Dimples," in *2018 Flow Control Conference*, Reston, Virginia: American Institute of Aeronautics and Astronautics, Jun. 2018. doi: 10.2514/6.2018-3528.

[49] **J. Tay, T. T. Lim, and B. C. Khoo,** "Drag Reduction with Diamond-shaped Dimples," in *AIAA Aviation 2019 Forum*, Reston, Virginia: American Institute of Aeronautics and Astronautics, Jun. 2019. doi: 10.2514/6.2019-3296.

International Journal of Engineering Research & Technology (IJERT)
ISSN: 2278-0181
Vol. 15 Issue 07 , July - 2026

[50] **J. Casey, P. King, and R. Sondergaard,** "Parameterization of Boundary Layer Control Dimples on a Low Pressure Turbine Blade," in *40th AIAA/ASME/SAE/ASEE Joint Propulsion Conference and Exhibit*, Reston, Virigina: American Institute of Aeronautics and Astronautics, Jul. 2004. doi: 10.2514/6.2004-3570.

[51] **C. Tay,** "Determining the Effect of Dimples on Drag in a Turbulent Channel Flow," in *49th AIAA Aerospace Sciences Meeting including the New Horizons Forum and Aerospace Exposition*, Reston, Virigina: American Institute of Aeronautics and Astronautics, Jan. 2011. doi: 10.2514/6.2011-682.

[52] **G. Gupta, E. Fernandez, M. Otto, and J. S. Kapat,** "Experimental and Numerical Investigation of Fully Turbulent Flow in a Rectangular Channel with Dimples and Protrusions," in *AIAA Propulsion and Energy 2019 Forum*, Reston, Virginia: American Institute of Aeronautics and Astronautics, Aug. 2019. doi: 10.2514/6.2019-4178.

[53] **R. Yadav and A. Bodavula,** "Numerical investigation of the effect of triangular cavity on the unsteady aerodynamics of NACA 0012 at a low Reynolds number," *Proc Inst Mech Eng G J Aerosp Eng*, vol. 236, no. 6, pp. 1064–1080, May 2022, doi: 10.1177/09544100211027042.

[54] **A. Bodavula, R. Yadav, and U. Guven,** "Numerical investigation of the unsteady aerodynamics of NACA 0012 with suction surface protrusion," *Aircraft Engineering and Aerospace Technology*, vol. 92, no. 2, pp. 186–200, Jan. 2020, doi: 10.1108/AEAT-01-2019-0022.

[55] **A. Bodavula, R. Yadav, and U. Guven,** "Stall Mitigation and Lift Enhancement of NACA 0012 with Triangle-Shaped Surface Protrusion at a Reynolds Number of 10^5," *SAE International Journal of Aerospace*, vol. 12, no. 2, pp. 01-12-02–0007, Nov. 2019, doi: 10.4271/01-12-02-0007.

[56] **S. Patial, P. Jain, P. Rawat, A. Bodavula, and R. Yadav,** "The study of the effect of the cavity on the flow over naca 0012 and selig 7003 aerofoil at low reynolds number using vortex shading method," in *AIAA Scitech 2020 Forum*, American Institute of Aeronautics and Astronautics Inc, AIAA, 2020. doi: 10.2514/6.2020-2218.

[57] **A. Bodavula and R. Yadav,** "NUMERICAL INVESTIGATION OF THE EFFECT OF THE SPANWISE GROOVE ON THE AERODYNAMIC CHARACTERISTIC OF A NACA 0012 AIRFOIL USING γ-REθt TRANSITION TURBULENCE MODEL," *International Journal of Fluid Mechanics Research*, vol. 49, no. 6, pp. 1–17, 2022, doi: 10.1615/InterJFluidMechRes.2022044435.

[58] **A. Bodavula,** "Effect of surface protrusions and cavities on airfoil aerodynamic efficiency at low Reynolds number," Sep. 2020.

[59] **K. Lodefier, B. Merci, C. De Langhe, and E. Dick**, "Transition Modelling With the SST Turbulence Model and an Intermittency Transport Equation," in *Volume 5: Turbo Expo 2003, Parts A and B*, ASMEDC, Jan. 2003, pp. 771–777. doi: 10.1115/GT2003-38282.

[60] **R. B. Langtry and F. R. Menter,** "Correlation-Based Transition Modeling for Unstructured Parallelized Computational Fluid Dynamics Codes," *AIAA Journal*, vol. 47, no. 12, pp. 2894–2906, Dec. 2009, doi: 10.2514/1.42362.

[61] **F. R. Menter,** "Two-equation eddy-viscosity turbulence models for engineering applications," *AIAA Journal*, vol. 32, no. 8, pp. 1598–1605, Aug. 1994, doi: 10.2514/3.12149.

[62] **J. van Ingen,** "The eN Method for Transition Prediction. Historical Review of Work at TU Delft," in *38th Fluid Dynamics Conference and Exhibit*, Reston, Virigina: American Institute of Aeronautics and Astronautics, Jun. 2008. doi: 10.2514/6.2008-3830.

[63] **C. Lada, M. Amir, C. Wong, and K. Kontis,** "Effect of Dimples on Glancing Shock Wave-Turbulent Boundary Layer Interactions," in *42nd AIAA Aerospace Sciences Meeting and Exhibit*, Reston, Virigina: American Institute of Aeronautics and Astronautics, Jan. 2004. doi: 10.2514/6.2004-1058.

[64] **W. F. J. Olsman and T. Colonius,** "Numerical Simulation of Flow over an Airfoil with a Cavity," *AIAA Journal*, vol. 49, no. 1, pp. 143–149, Jan. 2011, doi: 10.2514/1.J050542.

[65] **W. F. J. Olsman, A. Hirschberg, and R. R. Trieling,** "High Reduced Frequency Measurements on Airfoils with a Cavity," in *16th AIAA/CEAS Aeroacoustics Conference*, Reston, Virigina: American Institute of Aeronautics and Astronautics, Jun. 2010. doi: 10.2514/6.2010-3905.

[66] **P. Bissessur, X. Chen, and X. Zhang,** "Numerical Investigation of Subsonic 2D/ 3D Cavity Flows," in *42nd AIAA Aerospace Sciences Meeting and Exhibit*, Reston, Virigina: American Institute of Aeronautics and Astronautics, Jan. 2004. doi: 10.2514/6.2004-683.

[67] **P. W. Bearman and J. K. Harvey,** "Control of circular cylinder flow by the use of dimples," *AIAA Journal*, vol. 31, no. 10, pp. 1753–1756, Oct. 1993, doi: 10.2514/3.11844.

[68] **H.-C. Kim, H.-J. Kim, K. Nakahashi, T. Kato, and M. Tsunoda,** "Flow Fields Analysis Around Dimpled Cylinders with Spinning," in *44th AIAA Aerospace Sciences Meeting and Exhibit*, Reston, Virigina: American Institute of Aeronautics and Astronautics, Jan. 2006. doi: 10.2514/6.2006-1397.

[69] **Y. D. Cui and H. M. Tsai,** "Side Force Suppression by Dimples on Ogive-Cylinder Body at High Angles of Attack," in *46th AIAA Aerospace Sciences Meeting and Exhibit*, Reston, Virigina: American Institute of Aeronautics and Astronautics, Jan. 2008, p. 117508. doi: 10.2514/6.2008-368.